Title
Drosophila Pickpocket Channel Function in Courtship Behavior and Water Detection

Author
Thistle, Robert Stewart

Publication Date
2014

Peer reviewed|Thesis/dissertation

Drosophila Pickpocket Channel Function in Courtship Behavior and Water Detection

Robert Stewart Thistle

A dissertation submitted in partial satisfaction of the

requirements for the degree of

Doctor of Philosophy

in

Molecular and Cell Biology

in the

Graduate Division

of the

University of California, Berkeley

Committee:

Dr. Kristin Scott, Chair
Dr. Diana Bautista
Dr. Gian Garriga
Dr. Neil Tsutsui

Fall 2014

ABSTRACT

Drosophila Pickpocket Channel Function in Courtship Behavior and Water Detection

By

Robert Stewart Thistle

Doctor of Philosophy in Molecular and Cell Biology

University of California, Berkeley

Professor Kristin Scott, Chair

The gustatory system is primarily involved in feeding, allowing animals to distinguish nutrients from toxins. In the fruit fly *Drosophila melanogaster*, neurons of the gustatory system also function during egg-laying and courtship behavior, and are broadly involved in contact-mediated chemical recognition. Gustatory input in *Drosophila* occurs at structures called taste bristles, which are located on the proboscis, legs, wing margins, and ovipositor. Four chemosensory neurons are housed at the base of each bristle, three of which faithfully respond to specific modalities: sugars, bitters, or water. However, the function of the fourth chemosensory neuron, and the molecular mechanism responsible for its activation, remained elusive. Further, the physical properties of molecules responsible for sensory neuron detection is poorly understood.

Microarray analyses identified two genes encoding epithelial sodium channels (deg/ENaCs), PPK23 and PPK29, which show co-expression in the fourth taste neuron and are not expressed in any other tissues. These genes were exciting candidates for defining sensory neuron specificity, as a related channel, PPK28, confers water sensitivity to taste neurons. Initial expression studies revealed that these genes were co-expressed with the transcription factor *fruitless*, a critical molecule in the organization or sexual dimorphism in the fly. We hypothesized that PPK23 and/or PPK29 may function in pheromone detection and contribute to aspects of courtship behavior. The second chapter of this thesis demonstrates that these genes are imperative for mate discrimination during courtship, and the cells that express them serve as one of the earliest filters for the neural circuitry that leads to courtship enhancement or courtship inhibition. Finally, cells that express these genes respond directly to pheromone application in a male or female specific manner, suggesting the balance between attraction and repulsion at the sensory level may contribute to the overall decision of the organism.

How do pickpocket subunits contribute to mate discrimination behavior? The third chapter of this thesis is an exploration into subunit expression specificity. Calcium imaging studies suggest a heterogeneity in PPK23 cells. In order to separate attractive and repulsive circuits at the sensory level, we ascertained the behavioral genetic interactions between multiple subunits. We found that the population of cells expressing the subunit PPK25 responds exclusively to female pheromone molecules and is also critical for female receptivity. This provides direct genetic access to this component of the courtship circuit.

The function of pickpocket ion channels in signal transduction has yet to be demonstrated. PPK28 detects low osmolarity and has been shown to function when misexpressed in neurons as well as in heterologous systems. However whether it is a direct transducer of osmolarity or perhaps an amplifier of another protein is not known. In the fourth chapter, we delve into the mechanism of gating of pickpocket channels using PPK28 as a model. Our data suggest it is a direct transducer of mechanical force on the membrane and provides an exciting example to study other Deg/ENaC proteins in the role of mechanosensation.

Chapter 1

Chapter 2

Chapter 3

Acknowledgements

1. First I would like to thank my mentor Dr. Kristin Scott, whose unwavering support has seen me through my successes and my struggles. I have enjoyed our scientific discussions as well as our casual talks. She is the kind of mentor any graduate student would be lucky to have: accessible, kind, wise, and not afraid to try new ideas. If someone needs help learning a technique or writing a grant application, she is the first to volunteer. I want to thank you for your guidance, patience, and understanding (even during my most challenging semester!). The lab is an amazing place to learn and work because it has a wonderful leader.
2. I would also like to thank some of the Scott lab members who have left. I was initiated into the lunch group of Peter Cameron, Mike Gordon, Andrea Manzo, and Lisa Dennison my first year, all of whom provided countless hours of entertainment, advice, and venting time. Without Peter the *ppk23* project would not be possible and I am forever thankful that I could finish what you started. Mike and I often discussed reality television in the fly room when our dissections were not cooperating, and we still talk about Survivor from time to time. Andrea introduced me to the Bongo Burger salad, a meal I continue to eat every Monday. Finally, Lisa became my bay mate and confidant, and I'm reminded of her every time I open up one of her delicious canned jams.
3. A special thank you must also go to the current Scott lab members: Allan-Hermann Pool, Kevin Mann (both of whom I refuse to believe have just left), Colleen Kirkhart, Samantha Cheung, Ben Kallman, Christoph Scheper, Brendan Mullaney, Dave Harris, Heesoo Kim, Hyesoo Youn, Nick Jourjine, and Justine Chia. We always have great conversations and no one would hesitate to help one another. Thank you Colleen for being with me every step of the way, for making me laugh, for watching me break down and picking me back up, and for throwing some amazing birthday parties. Thank you Samantha for being an amazing bay mate, for encouraging me to cook new things, and for unfaultering friendship. I will miss baking cakes for you all.
4. To my friends outside of the lab: I cannot thank you enough. Julie Choe has pushed me through so many roadblocks I cannot even count them. From tiny pies to emergency Sunday morning hikes she has kept me afloat. Christopher Alvaro- no one quite understands me like you do, and I would venture to guess that the reciprocal is true. Nothing calms me down like a spontaneous sing-a-long (even if it is Taylor Swift). I also want to thank you for helping me grow into a more thoughtful and honest person. There are too many MCB students to thank but I will send a special thank you note to Livy Wilz, Kelly Schiabor, and Nicole Bieir.
5. None of this work would be possible without my thesis committee: Dr. Diana Bautista, Dr. Gian Garriga, and Dr. Neil Tsutsui. I have truly appreciated working with you and for all of your helpful advice during our meetings. I must especially thank Dr. Bautista, who mentored me as a rotation student and allowed me full access to her lab to perform

electrophysiology experiments as well as her post doctorate researcher Maurizio Pelligrino for technical advice.

6. I would also like to thank the Graduate Affairs Office for all of their service, support, and friendship. In particular Eric Bhulis and Berta Para have been lovely friends and wonderfully helpful.
7. I must also thank Aaron Smyth, my rock. You have seen me celebrate, lament, even go a bit crazy, but your encouragement never fails to keep me motivated. I look forward to what the future holds.
8. Finally, I must of course thank my parents. They have been my champions throughout life. I recall how challenging it was for all of us when I decided to move across the country. However, the weekly phone calls and occasional visits have kept our relationships strong. I love them both very much and wouldn't be where I am or who I am today without them.

Introduction

Overview – Sensory Processing

All forms of life must interact with the environment in order to survive. To do so, organisms have evolved a range of sensory systems that detect environmental stimuli and contribute to appropriate physiological and behavioral responses. These stimuli come in diverse forms, including light, sound, temperature, chemicals and compounds, and mechanical force. As a result, each sensory system for a particular stimulus has evolved specific mechanisms of detection, often unique to the ecological niche of an organism. Classically, the sensory systems can be categorized in two ways: those that detect changes in physical properties (vision, audition, touch, and proprioception) and those that detect environmental chemical substrates (olfaction and gustation). Although much is known about each system, the molecular participants and mechanism of transduction that lead to a cellular or behavioral change are still being elucidated. This thesis examines the ion channels that participate in *Drosophila melanogaster* gustation including their roles in behavior, cellular function, and mechanism of gating.

Chemical senses

Chemicals are all around us. They flavor our food, scent our homes, and even warn us of danger. The interaction between an organism and its chemical environment drives behavioral choice and contributes to survival. One can broadly divide the chemical senses into three subcategories: olfaction, gustation, and pheromone detection. Olfaction describes the detection of an odorant, or a small volatile molecule detectable by the olfactory system. Odorants can range in origin from plant perfumes to gasses released by microbes. In contrast, gustation is the detection of small, nonvolatile compounds detected by the gustatory system. These molecules are compounds such as sugars or salts. Pheromone detection, interestingly, can be volatile or nonvolatile. These compounds are released by individual organisms, detected by conspecifics, and often carry sexual information. Depending on the organism, pheromone molecules can be detected by the olfactory system, gustatory system, or similarly specialized systems like the rodent vomeronasal organ. Together, olfaction, gustation, and pheromone detection enable us to chemically understand our worlds.

Olfaction

As odorants are diverse in number, molecular shape, and size, the olfactory system has had to evolve in such a way to detect such a massive array of chemicals. In mammals, a large repertoire of seven transmembrane G-protein coupled receptors is expressed by sensory neurons that innervate the olfactory epithelium. Each odorant receptor neuron (ORN) expresses a single receptor allele. In mammals the number of OR genes can range from 800-1500, while fish can have as few as 100 (Buck and Axel, 1991; Touhara and Vosshall, 2009). The activity of each ORN represents the activation of a single odorant receptor. Each ORN class sends axonal projections into the olfactory bulb, wherein they synapse at a discreet structure called an olfactory glomerulus, so that the pattern of activated glomeruli reflects the pattern of activated receptors. Moreover, odorants are often detected by multiple ORs and some ORs have the potential to be broadly tuned, finely tuned, and even inhibited by their respective ligands,

increasing the power of the combinatorial detection code (Oka et al., 2004). Second-order olfactory neurons are mitral cells which each synapse onto a single glomerulus. From here, mitral cells carry the olfactory information to higher centers including the anterior olfactory nucleus, taenia tecta, olfactory tubercle, piriform cortex, anterior cortical amygdaloid nucleus, posterolateral cortical amygdaloid nucleus, and entorhinal cortex for further processing.

Drosophila use a similarly organized system in detecting volatile compounds. The sites of volatile detection on flies are the antennae and maxillary palps. Across these organs is an arrangement of bristles that capture odorants. Each bristle is innervated by olfactory sensory neurons (OSNs) which, like mammals, express a unique olfactory receptor out of a possible 62 (Touhara and Vosshall, 2009). In addition, all OSNs express an obligatory co-receptor termed Orco (OR83b). Although olfactory receptors in the fly were once thought to be GPCRs, they show little homology to mammalian olfactory receptors, suggesting they evolved independently. A more revised model posits that *Drosophila* ORs may function as ion channels (Benton et. al., 2006; Sato et. al.,2008). Ionotropic glutamate receptors (iGluRs) are also expressed in odor sensitive neurons devoid of ORs, which supports the notion that ion channels are more involved in chemical sensation than previously thought (Benton et. al., 2009). As in mammals, OSNs of a single class project to discreet glomeruli in a section of the central brain called the antennal lobe. From here, second order projection neurons carry odor information to higher brain regions like the mushroom bodies and lateral horn which are regions whose activity contributes to learned and innate behaviors.

Despite the differences in odor signal transduction in vertebrates and invertebrates the underlying logic of the system is still beautifully the same. The large number of receptors as well as the expression of a single receptor in each olfactory neuron gives the olfactory system powerful molecular discrimination.

Gustation

The gustatory and olfactory systems are similar in that they are chemically activated, however there are significant differences in molecular detection and organization. Organisms utilize the gustatory system to determine the palatability of food before deciding to consume. In mammals, taste is accomplished via taste receptor cells located in the taste bud of the tongue. These specialized epithelial cells can fire action potentials and information is carried through afferent nerves to the nucleus of the solitary tract in the brain stem. In mammals, taste cell classes can be activated by multiple modalities: sugars, bitter compounds, salts, amino acids, and CO_2.

As in olfaction, some tastant detection in mammals is mediated by G-protein coupled receptors in the taste receptor cells. For example, sugars and amino acids are detected by members of the Taste Receptor 1 (TR1) family. The heteromer comprised of T1R2 and T1R3 is a broadly tuned receptor for most sugars, whether natural or artificial. Similarly, the T1R1 and T1R3 heteromer detects L-amino acids such as L-glutamate. The Taste Receptor 2 family, of which there are 35 in mice, instead codes a large family of GPCRs involved in bitter detection. Unlike olfaction, T2Rs are monomeric, expressed together in a single cell type, and help the organism avoid consumption of things like toxins. Detection of these three modalities through their respective GPCRs leads to a signaling cascade that opens the cationic channel TRPM5,

depolarizing the taste cell. The other taste qualities of salt and acid are instead thought to be mediated by ion channel transduction. Taste receptor cells that respond to low salt express the epithelial sodium channel ENaC, and mutations in ENaCα lead to a loss of low salt taste attraction. Cells that express the transient receptor portential gene, PKD2L1, respond to acid exposure. However, genetic support for its response to acid is lacking, likely indicating that acid taste is accomplished by additional or multiple channels. Nevertheless, it is clear that gustation is organized in a modality specific manner at the sensory level.

Drosophila taste not with a tongue, but rather with multiple organs on the body: the proboscis, mouth parts, legs, wing margins, and ovipositor. Moreover, despite millions of years of evolution between flies and mammals, they can taste much the same range of things: sugars, bitter compounds, water, salt, and CO_2. Taste bristles contain 2-4 gustatory receptor neurons (GRNs) which respond in a modality specific manner, similar to mammalian taste receptor cells. *Drosophila* gustation is accomplished partially via gustatory receptors (GRs), of which there are 68. Like the ORs, GRs show divergent structure from canonical GPCRs and may function as ion channels. A third group of sensory neurons responds to low osmolarity solutions, and this is mediated through the ion channel PPK28, a Deg/ENaC (Cameron, et al. 2010). Finally, a fourth group of sensory neurons which express the ion channel PPK23 had no defined function. Calcium imaging experiments demonstrate that the modality segregation of tastants is maintained at the first relay point in the brain, the sobesophogeal zone (SEZ). As in mammals, the discovery of PPK28 and its role in taste behavior provided a framework with which to study the role of other ion channels in fly taste detection.

Unlike the olfactory system, the gustatory system is designed to categorize tastants into discreet modality catagories. How this bundling of sensory information is processed in the higher brain is not yet clear, but it will be exciting to determine the organization of the neural circuitry mediating gustation.

Pheromone detection

In addition to the main olfactory system, rodents also contain an accessory system which is largely associated with pheromone detection and mating behaviors. Pheromone odorants present in urine are detected by receptors expressed in the vomeronasal organ (VNO), a subsystem of the nasal cavity. In the epithelium of the VNO, distantly related G-protein coupled receptors (V1Rs, V2Rs, and V3Rs) are expressed by sensory neurons. The epithelium can be divided into an apical and basal layer, which express V1Rs and V2Rs respectively. Similar to the coding in main olfactory epithelium, these sensory neurons express a single receptor and project to the accessory olfactory bulb. Output neurons from this structure project to the limbic system. Genetic knock out studies of receptors or downstream signaling molecules causes courtship behavior defects in mice and demonstrate the critical role of the VNO in conspecific detection. Calcium imaging of intact VNO slices has also demonstrated tuning of VRs to volatile pheromones.

Male *Drosophila* detect both volatile and nonvolatile chemosensory pheromone molecules by the olfactory and gustatory systems, respectively. A variety of pheromone molecules, many of which are long chain cuticular hydrocarbons (CHCs), are known to mediate courtship in Drosophila. These CHCs are produced by cells called oenocytes and are expressed on the cuticle of the fly (Billeter, JC. et al., 2009). Many show a sexually dimorphic expression

pattern. For example, females show enrichment of CHCs with two double bonds, often 7,11 dienes, such as 7,11-heptacosadiene (7,11HD) and 7,11- nonacosadiene (7,11ND). This family of molecules has been shown to stimulate male courtship. In contrast, males show enrichment of monoenes such as 7-tricosene (7T) and 7-pentacosene (7P) (Ferveur, 2005; Jallon, 1984). This family of molecules acts to inhibit courtship by males and also increase the receptivity of females. Furthermore, there is emerging evidence that oxygenated, non-CHCs such as CH503 contribute to the inhibition of male courtship (Yew, JY. et al., 2009). In addition to characterization of these nonvolatile pheromones, a low volatile compound called cis-vaccenyl acetate (cVA) has been well demonstrated to be transferred from males to females during copulation and deter future male courtship towards the mated female. These compounds represent only a small, studied fraction of the complete pheromone profile of *Drosophila* and many others remain to be evaluated behaviorally.

Although *Drosophila* lack a discreet olfactory organ for pheromone detection, they nevertheless use volatile clues to make discriminatory mate choices during courtship behavior. Males release a low volatile compound called cVA during copulation which acts as a mating deterrent and aggression promoting pheromone. The olfactory neural circuitry for cVA has been well studied. Electrophysiology experiments demonstrate that cVA is detected by the olfactory sensory neurons (OSNs) which express either Or67d, Or65a, or Or67b, although Or67d and Or65a neurons appear to be the populations relevant for inhibition of courtship behavior. Or67d OSNs are *fruitless* positive and their connections beyond the antennal lobes are sexually dimorphic demonstrating an anatomical and physiological mechanism to influence sexually dimorphic behavior through olfaction (Datta et al., 2008; Ruta et al., 2010; Stockinger et al., 2005). This impressively mapped circuit, however, represents only one channel of stimuli that an organism receives during a behavior.

Identification of Pickpocket ion channels in chemosensory neurons

The *ppk23, ppk29,* and *ppk28* genes are three of 31 annotated pickpocket genes in the fly, belonging to a family of genes called Degenerin/Epithelial Sodium Channels (DEG/ENaCs). Other channels from this gene family contribute to diverse cellular functions and include the mammalian proton activated ion channels (ASICs) and *C. elegans* mechanically activated ion channels (MECs). All DEG/ENaC proteins share similar topographic features, including two transmembrane domains, a variable external domain, and two short internal termini. Crystal structure analysis has demonstrated that three DEG/ENaC subunits assemble to form a single channel, and that channels can be comprised of either homomeric or heteromeric partners. Furthermore, electrophysiological studies have demonstrated that DEG/ENaCs are non-voltage gated, sodium selective, and amiloride sensitive channels. Consequently, these genes represent exciting candidates with which to examine genetic, cellular, and structural function.

Previous work in our lab identified multiple *ppk* transcripts as enriched in *Drosophila* gustatory tissue, including *ppk28, ppk23,* and *ppk29.* Expression studies uncovered that these ion channels are exclusively in GRNs and lead to the investigation of their role in tastant detection. *ppk28* was shown to be crucial for water detection, as it was expressed in water sensitive neurons and mutants showed water consumption defects. Additional misexpression, calcium imaging, and cellular pharmacological experiments revealed that *ppk28* is the molecular sensor for low tonicity, capable of functioning in neurons normally sensitive to other modalities

as well as mammalian tissue culture cells. This unusual ability, not normally seen in reconstitution of GRs, for instance, lead us to explore how this channel could be activated.

Similar expression studies revealed that *ppk23* and *ppk29* were co-expressed in a significant portion of cells without an obvious modality. Despite exhaustive screens for taste behavior defects, the function of this cell type and the role these channels played in gustation remained elusive. Consequently, upon the observation that some projections were sexually dimorphic, we vigorously tested the role of these cells and ion channels in pheromone detection and courtship behavior.

Concluding Remarks

A fundamental question in neuroscience asks how organisms employ molecules, neurons, and neural circuits to translate the physical world into a perception. This thesis first explores how *Drosophila melanogaster* utilize gustatory neurons to identify appropriate mates. We show that the neurons expressing the ion channel genes *ppk23*, *ppk29,* and *ppk25* have crucial roles in courtship behavior. These neurons respond to non-volatile pheromone molecules present on the surface of flies and the specific expression of each ion channel is required for male/female discrimination. In order to better understand how these ion channels transduce signals, the second portion of this thesis investigates how PPK28, a water sensitive ion channel, is activated. We demonstrate that this channel detects mechanical force applied to cellular membranes and define key domains necessary for this detection. Together, these studies uncover new information regarding sensory neuron identity as well as ion channel function in the fly and provide new genetic and molecular entry points into studying the mechanics of sensory processing.

Chapter 1:
Contact Chemoreceptors Mediate Male-Male Repulsion and Male-Female Attraction during Drosophila Courtship

Preceding Remarks

In this chapter we investigate the role of pickpocket ion channels in *Drosophila* contact chemosensation. These data have previously been published (Thistle et. al., 2012), and are reproduced here with author permission. I performed a majority of the experiments including expression studies, behavior, calcium imaging, and co-wrote the manuscript. Peter Cameron initiated the project, generated fly strains, performed expression studies, and gave valuable feedback on the manuscript. Azeen Ghorayshi assisted with behavior experiments and data analysis. Lisa Dennison contributed to generating fly strains and expression studies. Kristin Scott performed expression studies, co-wrote the manuscript, and supervised the project.

In the final portion of this chapter we expand on our knowledge of the molecular components involved in *Drosophila* contact chemosensation. These data have been previously published (Vijayan, et al., 2014) and were in collaboration with Dr. Claudio Pikielney's laboratory at Dartmouth (Figure 8., and Additional Findings). They are summarized and reproduced here with author permission, highlighting the experiments I performed. I have also briefly included a conclusion of the remainder of the study, with which I assisted, but did not perform. For this project I generated calcium imaging data, advised behavioral experiments, performed statistical analysis, and edited the manuscript. Vinoy Vijan performed the majority of additional experiments and co-wrote the manuscript. Elena Starostina and Tong Liu assisted with behavioral experiments and expression studies. Claudio Pikielny co-wrote the manuscript and supervised the project.

Summary

The elaborate courtship ritual of Drosophila males is dictated by neural circuitry established by the transcription factor Fruitless and triggered by sex specific sensory cues. Deciphering the role of different stimuli in driving courtship behavior has been limited by the inability to selectively target appropriate sensory classes. Here, we identify two ion channel genes belonging to the degenerin/epithelial sodium channel/pickpocket (ppk) family, *ppk23* and *ppk29*, which are expressed in fruitless-positive neurons on the legs and are essential for courtship. Gene loss-of-function, cell-inactivation, and cell-activation experiments demonstrate that these genes and neurons are necessary and sufficient to inhibit courtship toward males and promote courtship toward females. Moreover, these cells respond to cuticular hydrocarbons, with different cells selectively responding to male or female pheromones. These studies identify a large population of pheromone-sensing neurons and demonstrate the essential role of contact chemosensation in the early courtship steps of mate selection and courtship initiation.

Introduction

Innate behaviors, from egg-rolling in geese to the honeybee waggle dance, are executed by genetically programmed neural circuits that are triggered by specific sensory cues. The *Drosophila* courtship ritual is comprised of a sequence of stereotyped behaviors that culminates in copulation, essential for propagation of the species. Courtship has emerged as a model for deciphering the neural basis of innate behavior because of its tight genetic control by the transcription factor Fruitless (Gill, 1963; Hall, 1978; Ito et al., 1996; Ryner et al., 1996). However, the sensory cues and neurons that initiate courtship behavior are only beginning to be elucidated.

Courtship involves a complex sequence of actions by the male. The male orients towards a female, chases her, taps her abdomen with his forelegs, plays a courtship song by extending and vibrating a single wing, contacts the ovipositor with his proboscis and finally mounts before copulation (Hall, 1994). This stereotyped behavior is dictated by the male-specific splice form of Fruitless, Fru^M (Goodwin et al., 2000; Ryner et al., 1996). *fru* mutants show reduced male-female courtship and enhanced male-male courtship (Ryner et al., 1996; Villella et al., 1997). Moreover, transgenic studies in which fru^M was selectively expressed in females caused them to perform nearly all aspects of male courtship (Demir and Dickson, 2005; Manoli et al., 2005).

Fru^M is found in ~1500 neurons in the fly brain that mark neural circuitry for courtship behavior (Lee et al., 2000; Manoli et al., 2005; Stockinger et al., 2005). Fru^M labels a pathway of synaptically connected neurons that detect sex-specific olfactory cues (Datta et al., 2008; Ruta et al., 2010; Stockinger et al., 2005). In addition, five different classes of Fru^M neurons elicit courtship song, suggesting that they comprise male-specific song circuitry (von Philipsborn et al., 2011).

In addition to sex-specific neural circuitry governed by Fru^M, appropriate courtship requires that males sense cues that trigger courtship toward females and prevent non-productive courtship toward males. Long-chain cuticular hydrocarbons (CHCs) produced by specialized cells called oenocytes (oe) act as non-volatile pheromones to trigger sex-specific behavior (Billeter et al., 2009; Ferveur, 2005; Ferveur et al., 1997). Flies lacking oenocytes (oe-) fail to evoke appropriate courtship behavior in wild-type males, indicating that cuticular hydrocarbons are an essential sensory component for courtship (Billeter et al., 2009). Female CHCs are enriched for 7,11-heptacosadiene (7,11-HD) and 7,11-nonacosadiene (7,11-ND), compounds that stimulate male courtship (Ferveur, 2005; Jallon, 1984). In contrast, male CHCs are enriched for 7-tricosene (7T) and 7-pentacosene (7P) (Ferveur, 2005; Jallon, 1984). In addition, a volatile hydrocarbon not produced by oenocytes, cis-vaccenyl acetate (cVA), is enriched in males (Butterworth, 1969). These compounds represent only a small, studied fraction of the complete hydrocarbon profile of *Drosophila* (Everaerts et al., 2010; Yew et al., 2009).

Despite the diversity of pheromones, only a handful of receptors and cell types have been implicated in pheromone sensing. Both olfactory and gustatory neurons mediate pheromone detection, with olfactory neurons detecting volatile cues and gustatory neurons sensing contact-mediated cues. The best-characterized olfactory receptor-ligand pair is Or67d-cVA (reviewed in Vosshall, 2008). The gustatory receptor genes *Gr32a* and *Gr33a* encode putative pheromone

receptors for contact mediated male-male repulsion, as mutants show enhanced courtship of beheaded males (Miyamoto and Amrein, 2008; Moon et al., 2009). Additionally, *Gr68a*, *Gr39a* and the ion channel gene, *ppk25*, have been implicated in male-female attraction (Bray and Amrein, 2003; Ejima and Griffith, 2008; Lin et al., 2005; Watanabe et al., 2011). The pheromones that these candidate receptors recognize and their relationship to Fru^M neurons have not been established.

The subtle phenotypes seen upon compromising small subsets of sensory neurons contrast with the dramatic defects observed when sex-specific circuitry or pheromone cues are absent. This suggests that additional sensory populations are required to evaluate potential mates. Contact-mediated recognition occurs via chemosensory bristles on the proboscis, internal mouthparts, legs, wing margins and ovipositor (Stocker, 1994). Most chemosensory bristles on the proboscis contain four neurons, three of which sense sugars, bitter compounds or water (Cameron et al., 2010; Chen et al., 2010; Thorne et al., 2004; Wang et al., 2004). However, the modality sensed by the fourth population of gustatory neurons and the functional and behavioral relevance of this cell type is not clear.

Here, we identify two ion channel genes, *ppk23* and *ppk29*, that are co-localized in the fourth population of gustatory neurons on the proboscis and in Fru^M-positive leg neurons. Gene loss-of-function, cell inactivation and cell activation experiments demonstrate that these genes and neurons are essential for recognition of males and females at early courtship steps. These studies identify a large population of chemosensory neurons responding to cuticular hydrocarbons and demonstrate the essential role of contact chemosensation in mate selection and courtship initiation.

Results

ppk23 and *ppk29* are specifically expressed in gustatory neurons

We previously performed a microarray-based screen for genes enriched in taste neurons (Cameron et al., 2010). Three taste-enriched genes are members of the degenerin/epithelial sodium channel (Deg/ENaC) family. *ppk28* is expressed in gustatory neurons that mediate water taste detection (Cameron et al., 2010). The other two genes are *ppk23* and *CG13568*. *CG13568*, which we name *ppk29*, contains 24% predicted amino acid identity to *ppk23*. Because Deg/ENaC channels are important for detection of a variety of stimuli including water, sodium, acids, mechanosensory stimuli and peptides (Mano and Driscoll, 1999), we examined whether *ppk23* or *ppk29* participates in gustatory detection.

To visualize expression of *ppk23* and *ppk29*, we generated transgenic flies to drive expression of reporters under the control of putative promoters, using the Gal4/UAS system. *ppk23-Gal4* and *ppk29-Gal4* drove expression of GFP in neurons on the proboscis, all legs and wing margins in both sexes (Figure 1A, Figure S1A and not shown). Moreover, axonal projections extended to the subesophageal ganglion (SOG), the primary taste relay (Figure 1A and Figure S1A). No expression of *ppk23* or *ppk29* was detected outside of gustatory sensory neurons.

Two-color *in situ* hybridization experiments with *ppk23* and *ppk29* demonstrated that both genes were co-expressed in the same proboscis population (93% [92/99] *ppk29* neurons expressed *ppk23*, 72% [92/128] *ppk23* neurons contained *ppk29*) (Figure 1B). In contrast, *ppk29-Gal4* labeled far fewer cells than *ppk23-Gal4* per labellum (*ppk29-Gal4*=5+/-2, *ppk23-Gal4*=22+/-2, n=10, t-test $P=e^{-21}$), suggesting that the *ppk29-Gal4* line under-represents *ppk29* expression, limiting its usefulness. However, *ppk23-Gal4* faithfully recapitulated *ppk23* endogenous expression (84/93 [90%] *ppk23-Gal4* neurons expressed *ppk23*, 84/84 [100%] *ppk23* neurons expressed *ppk23-Gal4*) (Figure S1B). These data show that *ppk23* and *ppk29* are largely co-expressed and that *ppk23-Gal4* reproduces *ppk23* expression.

Which cells express *ppk23* and *ppk29*? Previous studies have identified three different taste cell populations in the proboscis, including sugar-sensing cells labeled by Gr64f (Dahanukar et al., 2007), bitter sensing cells labeled by Gr66a (Thorne et al., 2004; Wang et al., 2004) and water sensing cells labeled by Ppk28 (Cameron et al., 2010; Chen et al., 2010). Another population marked by *ppk11-Gal4* has been proposed to mediate salt taste (Liu et al., 2003b); however, *ppk11-Gal4* is found in support cells in the adult (Figure S1C). Co-expression studies revealed that *ppk23* was not in sugar- or water-sensing cells (Figure 1B). A few Ppk23-positive cells were also Gr66a-positive (9 cells), but these represented only a small fraction of all Ppk23-positive (9/37) or Gr66a-positive cells (9/69) (Figure 1B). Two-color immunohistochemistry confirmed these results (Figure S1 DE). These analyses demonstrate that *ppk23* and *ppk29* mark an uncharacterized population of gustatory neurons in addition to a few bitter cells, suggesting that these neurons detect a novel taste modality.

ppk23 is expressed in fru^M-positive neurons on the legs

Although *ppk23-Gal4* is expressed in the same number of proboscis neurons in males and females (male=22+/-2 neurons, female=21+/-2 neurons, n=5/sex, t-test P=0.4), we found that it is expressed in twice as many leg neurons in males than females (first three tarsal segments of foreleg, male=26+/-1 neurons, female=14+/-0 neurons, n=4/sex, t-test P=0.004; Figure 1A). In addition, axonal projections from the forelegs are sexually dimorphic: male foreleg axons cross the ventral nerve cord midline whereas female axons do not (Figure 2A). Previous studies have shown that the transcription factor Fru^M is expressed in leg gustatory neurons and confers this male-specific axon projection pattern (Mellert et al., 2010), indicating that *ppk23* might be co-expressed with Fru^M and mark sexually dimorphic sensory neurons.

Double-labeling experiments showed that *ppk23-Gal4* and fru^{P1}*-LexA* (marking Fru^M cells) were co-expressed in leg sensory neurons, with almost complete overlap in expression (97% overlap; 66/68 cells) (Figure 2B). In the legs, *ppk23-Gal4* and fru^{P1}*-LexA* mark more than one cell underneath a bristle, consistent with previous studies of fru^{P1}*-LexA* (Mellert et al., 2010). Candidate pheromone receptors Gr32a and Gr68a target different cells (Figure 2C). In addition, markers for sugar, bitter and water did not co-label fru^M-positive leg neurons (Figure 2C). In contrast to leg expression, *ppk23-Gal4* and fru^{P1}*-LexA* were not co-expressed in the proboscis. Instead, fru^{P1}*-LexA* appears to label the mechanosensory neuron based on morphology and lack of marker co-expression (Figure S2) (Falk et al., 1976). Despite the differential labeling in the proboscis, the co-expression with fru^{P1}*-LexA* in the legs raised the possibility that *ppk23* might label sensory elements of the courtship circuit.

Δ*ppk23* and Δ*ppk29* mutants display courtship defects

To test the role of *ppk23* and *ppk29* in sensory detection, we generated gene deletions by FLP-recombination target (FRT) mediated trans-recombination (Parks et al., 2004). Δ*ppk23*, Δ*ppk29* flies showed no significant defects in detection of sugars, bitter compounds, salt or water using proboscis extension assays (Figure S3).

Because *ppk23* and *ppk29* are expressed in sexually dimorphic, fru^M-positive leg neurons, we hypothesized that they might mediate pheromone detection during courtship behavior rather than food recognition. Mutant flies and isogenic w^{1118} controls were paired with wild-type males, wild-type virgin females and other mutant males in a courtship paradigm. Δ*ppk23* males showed vigorous courtship toward wild-type target males as measured by the number of unilateral wing extensions (Figure 3A). Moreover, when 6-9 Δ*ppk23* males were placed together in a chamber, they serially courted each other, forming long chains in which males followed each other and produced courtship song (Figure 3B). These dramatic defects were rescued by introduction of a *ppk23* transgene under the control of the *ppk23-Gal4* promoter into the mutant background. In contrast, Δ*ppk29* males showed no aberrant courtship toward other males. These phenotypes suggest that *ppk23* is required for the detection of an inhibitory signal present on males to prevent inappropriate male-male courtship.

Wild-type males will court target males lacking oenocytes, the cells that produce cuticular hydrocarbons (Billeter et al., 2009). This attraction is due to an absence of inhibitory hydrocarbons on the target, unmasking an attractive olfactory cue (Wang et al., 2011). We tested

whether Δ*ppk23* male-male courtship relies on olfactory information and found that Δ*ppk23* males lacking antennae showed a complete loss of male-male courting behavior (Figure 3AB). This reinforces the model that Δ*ppk23* males fail to detect inhibitory cuticular hydrocarbons on other males and instead detect an attractive cue via the olfactory system.

We tested if *ppk23* and *ppk29* are also important for courtship toward wild-type virgin females. In a thirty minute trial, both Δ*ppk23* and Δ*ppk29* males courted with reduced frequency, longer latency and often failed to court (Figure 3CD and Figure S4). Importantly, reintroduction of *ppk23* into Δ*ppk23* flies rescued the courtship defects. Similarly, reintroduction of *ppk29* into Δ*ppk29* flies using *ppk23-Gal4* rescued the behavioral phenotypes. This argues that *ppk29* is expressed in *ppk23* cells. Together, these experiments suggest that both *ppk23* and *ppk29* are required for the detection of excitatory signals present on females during courtship.

As *ppk23* and *ppk29* are related members of the Deg/ENaC ion channel family, we wondered whether overexpression of one might compensate for the loss of the other. Introduction of *UAS-ppk29* into Δ*ppk23* using *ppk23-Gal4* failed to rescue the courtship defects (Figure 3). Similarly, the responses of Δ*ppk29* males containing *UAS-ppk23* and *ppk23-Gal4* were identical to the responses of Δ*ppk29* males (Figure 3). Thus, the two genes have non-redundant functions in courtship.

Silencing or activating *ppk23* neurons elicits opponent courtship behaviors

To confirm and extend the mutant studies, we examined whether silencing *ppk23* cells recapitulates the mutant phenotype. We expressed tetanus toxin light chain (*UAS-TNT*) in *ppk23-Gal4* cells to block synaptic transmission (Sweeney et al., 1995) and examined courtship behavior. Similar to Δ*ppk23* males, males with *ppk23* cells silenced increased single wing extensions to wild-type males (Figure 4A). They also increased courtship latency and decreased wing extensions toward wild-type females (Figure 4B and Figure S4). These findings are consistent with the Δ*ppk23* studies.

Our expression studies indicated diversity in cell-types that contain *ppk23*. *ppk23* is co-expressed with *Gr66a* in a few proboscis neurons and co-expressed with fru^{M} in leg neurons but not proboscis neurons. To decipher which neurons contribute to the courtship defects assayed, we inactivated subsets of *ppk23* cells. *lexAop-Gal80* transgenic flies were generated to inhibit expression of Gal4-dependent reporters in *Gr66a-LexA* cells or fru^{P1}*-LexA* cells. *ppk23-Gal4, UAS-TNT* flies in which *Gr66a* cells expressed *Gal80* showed male-male and male-female courtship defects similar to *ppk23-Gal4, UAS-TNT* flies (Figure 4AB). In contrast, *ppk23-Gal4, UAS-TNT* flies with fru^{M} cells containing *Gal80* showed no courtship to males and normal courtship to females, similar to wild-type controls (Figure 4AB). This argues that the *ppk23,* fru^{M}-positive leg neurons are required for appropriate courtship and that the *Gr66a* cells do not significantly contribute.

The loss-of-function studies indicate that *ppk23* cells are necessary to inhibit male-male courtship and promote male-female courtship. If *ppk23* cells detect pheromones and actively mediate courtship behavior, then inducible activation of *ppk23* cells may be able to drive

courtship even in the absence of pheromonal cues. Courtship assays were performed with oe- flies as targets, as they lack the majority of cuticular hydrocarbons and wild-type males court both male and female oe- flies (Billeter et al., 2009). The temperature-gated cation channel dTRPA1 was expressed in *ppk23-Gal4* neurons to conditionally activate these neurons upon thermal increases (Hamada et al., 2008). At permissive temperature, *ppk23-Gal4, UAS-dTRPA1* males and controls courted oe- males and females, as expected (Figure 4C). When dTRPA1 was activated at 30^{o}C, *ppk23-Gal4, UAS-dTRPA1* males reduced courtship toward oe- males and increased courtship toward oe- females (Figure 4C). When paired with oe+ flies (containing pheromones) at 30^{o}C, *ppk23-Gal4, UAS-dTRPA1* males did not court oe+ males but increased courtship toward oe+ females (Figure 4D). This suggests that endogenous male cues prevent male-male courtship, as expected. In addition, the enhanced attraction towards oe+ females suggests that endogenous female cues may be limiting and not maximally activate *ppk23* cells.

These results demonstrate that activation of *ppk23* cells drives appropriate courtship behavior. The observation that *ppk23* cell activity inhibits male courtship yet triggers female courtship in flies lacking cuticular hydrocarbons implies that other sex-specific cues act in concert with *ppk23* cell activation to select gender-appropriate behavior. Consistent with this, *ppk23-Gal4, UAS-dTRPA1* and control males do not show any courtship behavior without visual and olfactory inputs (Figure S4). This demonstrates the importance of other sensory cues in triggering courtship behavior. We hypothesize that these other cues assist the fly when all *ppk23* cells are active, likely producing conflicting pheromone signals.

ppk23 and *ppk29* are required for behavioral responses to multiple pheromones

The courtship defects suggest that *ppk23* and *ppk29* may participate in detection of male inhibitory pheromones and female excitatory pheromones. To test the specificity of *ppk23* cells in pheromone detection, behavioral approaches were used to examine the response of Δ*ppk23* and Δ*ppk29* males to cuticular hydrocarbons (Billeter et al., 2009; Wang et al., 2011). 7T and cVA are inhibitory compounds on males and 7,11-HD, and 7,11-ND are excitatory compounds on females (Ferveur, 2005; Jallon, 1984). 7P is abundant on males, with more complex roles in courtship (Ferveur, 2005; Jallon, 1984; Wang et al., 2011). Δ*ppk23*, Δ*ppk29* and control males were paired with oe- males painted with 7T, 7P or cVA. Whereas controls reduced courtship to oe- males in the presence of these compounds as expected, the responses of Δ*ppk23* and Δ*ppk29* were not significantly affected (Figure 5A). Male-male courtship toward oe- males was due to an olfactory cues as loss of the antenna in control, Δppk23 or Δppk29 males abolished this behavior (Figure 5A). Additionally, controls increased courtship to oe- females painted with 7,11-HD, 7,11-ND or 7P, whereas Δ*ppk23* and Δ*ppk29* showed no change in behavior (Figure 5B). Thus, both Δ*ppk23* and Δ*ppk29* males behave as though they are blind to multiple pheromonal compounds.

Interestingly, both Δ*ppk23* and Δ*ppk29* showed decreased male-female courtship to oe- flies compared to control. This suggests that there are excitatory signals on oe- females that wild-type flies detect and mutants fail to recognize. Similarly, Δ*ppk23* males appear to show increased courtship to oe- males, although this difference is not significant. This suggests that there are inhibitory signals on oe- males that wild-type flies detect and mutants fails to recognize. These

signals may be residual pheromones due to incomplete ablation of oenocytes (Billeter et al., 2009) or non-oenocyte derived cues.

ppk23 cells respond to pheromones

We monitored calcium increases by G-CaMP imaging to assess whether *ppk23* cells directly sense pheromones. Responses were initially monitored from single leg neurons in tethered flies, as our behavioral studies indicated a central role for the *ppk23*-positive, fru^M-positive leg neurons in courtship. To evaluate whether *ppk23* cells respond to pheromones, we examined the response to mixes of five cuticular hydrocarbons (7P, 7T, cVA, 7,11-HD, 7,11-ND) dissolved in 10% ethanol. G-CaMP fluorescent increases were observed in male and female leg neurons to the pheromone mix but not to 10% EtOH alone (Figure 6A). Responses were dose-sensitive, with significant responses at 10 and 100 ng/μl. Additionally, bristles were tested for responses to sucrose, salt and quinine (Figure 6B). Cells did not respond to sucrose or salt. 6/27 cells responded to quinine; the high variance led to statistically insignificant responses. The pheromone mix activated *ppk23* cells from legs and proboscis for both sexes (Figure 6CD). These responses required *ppk23* and *ppk29*, as Δ*ppk23* and Δ*ppk29* cells did not respond to the hydrocarbon mix. Moreover, re-introduction of *ppk23* into Δ*ppk23* rescued the G-CaMP response, arguing that loss of the response is due to loss of *ppk23*. The decreased sensitivity of proboscis neurons to the pheromone mix as compared to leg neurons suggests that high concentrations may be required to activate these cells and/or that other compounds may optimally activate the cells.

To test whether *ppk23/ppk29* are sufficient to confer responses to pheromones, we misexpressed *ppk23/ppk29* in *ppk28* cells in a Δ*ppk28* background. These cells are water-sensing gustatory neurons but show no water responses in the absence of *ppk28* and serve as an "empty" gustatory neuron (Cameron et al., 2010). Misexpression of *ppk23/ppk29* failed to confer responses to the pheromone mix upon stimulation of leg or proboscis bristles (Figure 6E). The same *ppk23/ ppk29* constructs rescued mutant behavior and GCaMP responses in the Δ*ppk23/* Δ*ppk29* background, arguing that the constructs are functional. These studies suggest that additional components are required for pheromone sensitivity, although expression levels, folding or localization may limit the ability to assess function.

We next tested the response of *ppk23* leg neurons to individual compounds. Several chemosensory bristles on the leg are innervated by two *ppk23*-positive cells, providing the opportunity to monitor the response of both cells upon stimulation at the bristle tip. The two cells underneath a bristle showed remarkable specificity toward pheromones. One cell responded best to 7,11-HD and 7,11-ND and the other cell responded to 7P, 7T and cVA, with heterogeneity in the response to these compounds (Figure 7). Cells from males or females showed similar response profiles. Grouping one of the two cells under a bristle as "female-sensing" and the other as "male-sensing" based on maximal responses revealed a clear segregation of sex-specific responses (Figure 7BC). The G-CaMP imaging experiments argue that the *ppk23* cell population recognizes both male and female pheromones but that individual cells are tuned to a few compounds. Notably, cells generally responded to compounds from males or females but not both, arguing for sex-specific responses. Thus, the *ppk23* cell population likely represents the

majority of contact chemoreceptors for pheromones on the legs involved in male-male and male-female recognition.

Conclusion

In this study, we identify two ion channels, *ppk23* and *ppk29*, selectively expressed in uncharacterized contact chemosensory neurons and show that these genes and neurons are essential for inhibiting inappropriate courtship toward males and promoting courtship toward females. *ppk23* cells respond to either male or female pheromones and Δ*ppk23* cells do not respond. Several important findings emerge from this work: (1) Ppk ion channels are critical for pheromone detection in sensory cells; (2) pheromone detection by contact chemoreceptors is essential for very early courtship steps; (3) There are dedicated cells for pheromone detection that are distinct from sugar, bitter or water cells; (4) both males and females have gender-selective cells: one population responds to hydrocarbons produced by males and a different population responds to hydrocarbons produced by females. This work significantly advances our understanding of the detection of non-volatile pheromones.

The role of Ppk ion channels in pheromone detection

Ion channels of the Deg/ENaC family have been implicated in the detection of salts, acids, water, mechanosensory stimuli and peptides (Mano and Driscoll, 1999). In *Drosophila*, there are approximately 30 members of this family (Adams et al., 1998; Liu et al., 2003a). The founding member, pickpocket (Ppk) is thought to sense noxious mechanosensory stimuli (Zhong et al., 2010), Ppk11 and Ppk19 mediate salt taste detection in larvae (Liu et al., 2003b) and Ppk28 mediates water taste detection (Cameron et al., 2010; Chen et al., 2010). However, the majority of this family remains to be characterized.

Here, we identify *ppk23* and *ppk29* as co-expressed in uncharacterized neurons on the proboscis and in fru^M-positive chemosensory neurons on the leg. These two genes play critical roles in courtship behavior. Δ*ppk23* males increase courtship toward males and both Δ*ppk23* and Δ*ppk29* males decrease courtship toward females. Behaviorally, Δ*ppk23* and Δ*ppk29* fail to respond to individual male and female hydrocarbons. Moreover, *ppk23* cells respond to pheromone mixes whereas Δ*ppk23* and Δ*ppk29* cells do not. These studies argue that both *ppk23* and *ppk29* are essential for the recognition of both male and female pheromones.

The difference in behavior of Δ*ppk23* and Δ*ppk29* to males argues that the two genes have partially non-overlapping functions. The most parsimonious explanation is that Δ*ppk29* males, unlike Δ*ppk23* males, retain some ability to sense male inhibitory compounds. This suggests an underlying difference in expression or function of the two genes. The precise extent of co-expression is difficult to determine given the weak expression of the *ppk29-Gal4* line.

Do Ppk23 and Ppk29 detect pheromones, transduce pheromone signals or more indirectly influence pheromone detection by setting the membrane potential? Our current studies do not address this, but their selective expression in a subpopulation of chemosensory neurons and the inability of the two genes to cross-rescue argues for a specific function. As *ppk23* cells are heterogeneous in their response to individual hydrocarbons, it is unlikely that *ppk23* alone provides response specificity toward pheromones. Moreover, misexpression attempts in which *ppk23* and *ppk29* were expressed in "empty" gustatory neurons did not confer responses to

pheromones. Interpretations of the misexpression experiments are limited as expression levels, folding or localization may all impact function.

What components might be upstream of Ppk23/Ppk29 in pheromone detection? The two candidate pheromone receptors for which Gal4 lines have been generated, Gr32a and Gr68a, are not localized to *ppk23* neurons. *ppk25* has previously been implicated in male-female recognition but its expression has not been resolved (Ben-Shahar et al., 2010; Lin et al., 2005). Other members of the Deg/ENaC family of ion channels have not been shown to transduce signals downstream of G-protein coupled receptors (Mano and Driscoll, 1999). One possibility is that response specificity could be achieved either by the heteromultimeric composition of Ppk channels or by accessory binding proteins such as CheB42a, previously implicated in pheromone detection (Park et al., 2006). Alternatively, unidentified molecules may provide specificity.

Although the precise role of Ppks in pheromone detection remains to be examined, the demonstration that *ppk23* and *ppk29* are expressed in sexually dimorphic, fru^M-positive leg neurons and are essential for responses to male and female pheromones provides a strong foundation for future studies.

The role of contact chemoreceptors in courtship behavior

Courtship behavior is comprised of a series of behavioral subprograms that are executed in response to visual, auditory, olfactory and contact chemosensory cues (Greenspan and Ferveur, 2000; Hall, 1994). Teasing out the role of different sensory cues in driving courtship behavior has been limited by the ability to selectively target different classes of sensory neurons. Here, we identify a large population of pheromone-sensing neurons on the legs that co-express *ppk23* and fru^M, allowing us to selectively manipulate the contact chemosensory component of the *fruitless* circuit.

Contact chemoreceptors have largely been proposed to function in later stages of courtship during the foreleg tapping and proboscis contact steps, as these involve chemosensory organs (Bray and Amrein, 2003; Ferveur, 2005; Greenspan, 1995). In this study, we find that flies lacking *ppk23* or *ppk23* cell activity show behavioral defects at very early steps in the courtship process: they fail to distinguish males from females and delay or fail to initiate courtship of females. Recent studies on males with only a few residual chemosensory bristles found that they increased male-male courtship and decreased male-female courtship under dark conditions (Krstic et al., 2009), in line with our results. The defects in courtship initiation do not preclude a role in later steps such as foreleg tapping or proboscis contact but complicate evaluation. The very early defects in sex discrimination and initiation of courtship argue that contact chemoreceptors participate in male-female recognition prior to physical contact with other flies.

How does recognition occur at a distance? Pheromones that activate *ppk23* cells could potentially be volatile or sprayed by wings and deposited by legs, leaving lipid trails. As cuticular hydrocarbons have low volatility (Antony and Jallon, 1982), it is more likely that *ppk23*-positive cells sense deposited lipids. An interesting possibility is that transient pheromone trails may guide a male to a female, similar to pheromone trails that recruit ants to a food source.

Labeled lines for pheromone detection

In mammals, pheromones are detected by the vomeronasal organ and the olfactory epithelium, allowing animals to respond to diverse chemical cues signifying potential predators or mates (reviewed in Stowers and Marton, 2005). In *Drosophila*, subsets of olfactory and gustatory neurons are responsible for pheromone detection. In the olfactory system, three of ~50 glomeruli are fru^M-positive (Manoli et al., 2005; Stockinger et al., 2005), suggesting that they comprise a pheromone-specific subsystem. In the gustatory system, fru^M and *ppk23* are co-expressed in sensory neurons that are essential to promote courtship toward females and prevent inappropriate courtship toward males. These cells are distinct from those expressing markers for sugar, bitter or water-sensing cells, indicating that they form a pheromone-specific subsystem of the gustatory system. In the legs, these cells selectively respond to male or female pheromones, suggesting that there are sex-specific sensory cells. This argues that dedicated neurons for pheromone detection act as labeled lines in males to inhibit male-male courtship and initiate male-female courtship. The role of these sex-specific cells in females will be interesting to explore. Thus, the contact chemosensory system contains different cell populations tuned to sugars, toxins, water or other flies, extracting the essence for life from the environment.

Additional Findings

The F cell expresses *ppk25*

Multiple reports have indicated that members of the pickpocket ion channel family are required for the gustatory detection of *Drosophila* cuticular hydrocarbon pheromones. We previously showed that *ppk23* is expressed in pairs of gustatory bristles that also express *fruitless.* These cells have opponent response properties, with one cell responding best to stimulatory female pheromones (termed the "F cell") while the other responds best to inhibitory male pheromones (termed the "M cell"). However, molecular markers to define these cells and allow genetic access for the underlying circuit of courtship behavior were not available. Therefore, we performed calcium imaging to assess the response profile of *ppk25* neurons. This gene is only expressed in a subset of *ppk23* expressing neurons and we identify these as the F cells. Additional behavior experiments provide interesting insight into the behavioral role of *ppk25* neurons.

To evaluate the ligand specificity of ppk25 cells, expression of the genetically-encoded calcium indicator, G-CaMP3 (Tian, L. et al, 2009), was targeted using the ppk25-Gal4 driver (Starostina, E., et al., 2012). Single bristles on the front legs of both males and females were stimulated with two female pheromones that had been previously shown to stimulate the F (female-sensing) subset of ppk23-expressing cells (7,11-HD and 7,11-ND), and three compounds produced by males that stimulate M (male-sensing) cells (7-tricosene (7T), 7-Pentacosene (7P) and cVA) (Thistle, et al., 2012). As shown previously for F cells (Thistle, et al., 2012), ppk25-expressing cells in both males and females showed robust calcium responses to the female pheromones, 7,11-HD and 7,11-ND, but not to the male compounds, 7T, 7P or cVA (Fig. 1A). Importantly, this response requires ppk25, as ppk25 null mutants no longer responded to the female cues and targeted expression of ppk25 in mutants rescued this defect (Fig. 8A). To confirm that ppk25 is required in cells that detect female pheromones but not in those that detect male pheromones, ppk23-Gal4 was used to drive expression of G-CaMP3 in all pheromone-sensing cells in a ppk25 null mutant background. As described previously for flies with normal ppk25, ppk23-Gal4 labeled two cells under each bristle in ppk25 mutants. However, while one of these cells responded specifically to male compounds as previously described for M cells (Thistle, et al., 2012), the second cell, did not respond to female compounds as expected of F cells (Fig. 8B). Thus, ppk25 is essential for the recognition of courtship-stimulating pheromones produced by females but not of courtship-inhibiting pheromones produced by males.

Results summary

As calcium imaging data suggested a role for *ppk25* in sensing stimulatory female pheromone molecules, but not inhibitory male pheromone molecules, the authors sought to evaluate the role of *ppk25* in various behavioral paradigms. Consistent with previous results in the gene's requirement for normal male-female courtship behavior, but not courtship inhibition,

ppk25 mutant males failed to increase courtship when their pheromone-blank targets were painted with the stimulating pheromone 7-11HD. These mutants, however, suppressed courtship behavior when their pheromone-blank targets were painted with the inhibitory compound 7T. These data argue that *ppk25* functions exclusively in the F cell during behavior. RNAi knockdown of *ppk25* and neural silencing experiments supported this conclusion. Interestingly, targeted rescue of *ppk23* in *ppk25* expressing cells using a *ppk25-Gal4* transgene was able to rescue the male-female courtship phenotype, but not the male-male courtship phenotype, of *ppk23* mutants. This result is consistent with our original model of two functional types of pheromone sensing cells: one that expresses *ppk23* and *ppk25*, responds to stimulatory female compounds, and a second that expresses *ppk23* and not *ppk25*, which responds to inhibitory male compounds.

The authors also investigate the role of these ion channels in female receptivity, an area of courtship that has received less attention. Mutations in either *ppk23* or *ppk25* greatly inhibited the receptivity of female flies, which could be rescued by transgenic expression of the channels, and was not dependent on the mating activity of their male counterparts. Neural silencing experiments yielded similar results. These data are interesting in that *ppk25* neurons contribute to courtship stimulation in both sexes, despite being tuned to female compounds physiologically. It is possible that these sensory neurons respond to molecules not yet tested, or that downstream neural substrates influence female behavior in a sexually dimorphic way. Nevertheless, these additional behavioral experiments represent one of the first explorations into the physiological role of pickpocket ion channels in female mating choice.

Experimental Procedures

Experimental Animals

P element-mediated transformations of w^{1118} were performed using standard techniques (Genetic Services Inc.) Lines used: *UAS-TNT* (Sweeney et al., 1995); *UAS-mCD8::GFP* (Lee and Luo, 1999); *UAS-CD2::GFP* and *lexAop-CD2::GFP* (Lai and Lee, 2006); *UAS-TRPA1* (Hamada et al., 2008); *Gr64f-Gal4* (Dahanukar et al., 2007), *Gr66a-Ires-GFP* (Wang et al., 2004), fru^{P1}-*LexA* (Mellert et al., 2010), *ppk28-Gal4* (Cameron et al., 2010), *Gr5a-Gal4* (Chyb et al., 2003), *Gr68a-Gal4* (Bray and Amrein, 2003), *Gr66a-Gal4* and *Gr32a-Gal4* (Scott et al., 2001).

Generation of transgenes

Transgenes were generated from PCR amplification and cloning into pCaSpeR-AUG-Gal4 (Vosshall et al., 2000), pUAST, pLOT or LexA-pCaSpeR. Constructs were verified by sequencing. See Supplemental Experimental Procedures for details.

Generation of deletion mutants

Δ*ppk23* and Δ*ppk29* were generated by FLP-FRT mediated recombination (Parks et al., 2004). See Supplemental Experimental Procedures for details.

In situ hybridization

Double label *in situ* hybridization experiments were performed as described (Fishilevich and Vosshall, 2005).

Immunohistochemistry

Staining was performed as described (Wang et al., 2004).

Mutant Courtship Behavior

Courtship behaviors were performed as described (Demir and Dickson, 2005; Villella et al., 1997), with modifications detailed in Supplemental Experimental Procedures.

Ligand Painting Behavior

Oe- male and female target flies were generated as previously described (Billeter et al., 2009). oe- females were pierced through the head to prevent copulation (Gailey et al., 1984). 0.2μg of pheromone dissolved in hexane (7,11-HD, 7,11-ND, 7T and 7P) or ethanol (cVA) was applied to filter paper and evaporated. 8-16 oe- flies were gently vortexed with the filter paper twice for 20 seconds, roamed for ~30 minutes, then were transferred to a fresh vial 24 hrs prior to courtship assays.

G-CaMP Imaging

See Supplemental Experimental Procedures.

Extended Experimental Procedures

Generation of transgenes

ppk23-Gal4 was generated with 2.695 kb upstream fragment (17463170-17465864, GenBank NC_004354.3), cloned into pCaSpeR-AUG-Gal4 (Vosshall et al., 2000).
ppk29-Gal4 was generated with a 3.612 kb fragment (19942397-19946008, GenBank NT_033778.3), cloned into pCaSpeR-AUG-Gal4 (Vosshall et al., 2000).
UAS-ppk23 was generated by amplifying *ppk23* (variant RA, NM_132992) and cloning into pUAST.
UAS-ppk29 was generated by amplifying *CG13568* (variant RD, NM_001103972, bp 283-1674) and cloning into pUAST.
ppk28-LexA was generated by PCR amplification of the 1.004 kb promoter fragment in *ppk28-Gal4* (Cameron et al., 2010) and cloning into a *LexA-CaSpeR* vector.
LexAop-Gal80 was generated by amplifying the *Gal80* open reading frame from *tub>Gal80>* (Gordon and Scott, 2009) and cloning into pLOT.

Generation of deletion mutants

ppk23 mutants were generated by FLP-FRT mediated recombination between *piggybac* transposons d04369 and e03639, removing 8.284 kb surrounding *ppk23*, including a 3' fragment of *CG8465*, with no known function. *ppk29* mutants were generated by FLP-FRT mediated recombination between *piggybac* f06838 and f02213, removing the first two and part of the third exons as well as 331-bp 5' of the gene affecting *cg13563*, with no known function. Deletions were confirmed by sequencing.
Flies were backcrossed to 6-7 times to an isogenic w^{1118} fly strain (Exelixis strain A5001, BL6326). Backcrossed flies were *Δppk23*, *Δppk29*, *ppk23-Gal4*, *ppk29-Gal4*, *UAS-ppk23* and *UAS-ppk29*.

Mutant Courtship Behavior

Males were raised in isolation for 4-10 days post eclosion and paired with a sex-segregated, group-housed *Canton-S* target fly. Target virgin females were aged 2-5 days and target virgin males aged 4-10 days. Flies were transferred by gentle aspiration into a chamber designed from a Falcon 48 Well Plate, with Fluon-painted walls. The chamber contained a small piece of grape juice agarose. Courtship was recorded with a Sony DCR-HC38 Camcorder and captured using Windows Media Encoder. For male-male paradigms, genotypes were distinguished by dotting one fly with a water-soluble marker. All experiments were scored blind to genotype. Experiments were done under light conditions at room temperature. Male-male assays were recorded for 20 minutes; male-female assays were recorded for 30 minutes.

For assays with wild-type females (Figure 3), courtship assays were terminated upon copulation. Thus, wing extensions for male-male courtship and male-female courtship in Figure 3 are not comparable. Male-male courtship does not proceed to copulation and courtship song occurs throughout the 20 minute assay. Male-female courtship assays proceed to copulation and

terminate at different times. Therefore, the total number of wing extensions was divided by the copulation time in male-female assays to give a number of extensions/minute.

For chaining experiments, groups of 6-9 males were filmed in a 10 minute assay. Index of chaining equals (time 3 or more males serially court)/ total time.

For dTRPA1 experiments, males were assayed at 18^{o}C and 30^{o}C with oe- male and female targets. oe- flies were generated as previously described (Billeter et al., 2009). To prevent copulation, oe- females were pierced through the posterior portion of the head with forceps, rendering them immobile but upright (Gailey et al., 1984).

G-CaMP Imaging

Flies expressing *UAS-GCaMP3* and *ppk23-Gal4* were immobilized and forelegs tethered using parafilm, exposing the distal three tarsal segments. Pheromone mixes of 7,11-HD, 7,11-ND, 7T, 7P and cVA in 10% EtOH were applied to single bristles for 30s. 1M sucrose, 1mM quinine, and 1M NaCl were delivered followed by 10% ethanol alone. Responses were recorded on a 3i Spinning Disk confocal microscope with fixed stage. The maximum change in fluorescence ($\Delta F/F$) was calculated by dividing the peak intensity change by the average intensity four seconds immediately prior to stimulation.

For single pheromone studies, bristles were presented with 10% hexane, followed by randomized 7,11-HD, 7,11-ND, 7T, 7P and cVA (10ng/μl in 10% hexane), concluding with a mix of the five pheromones. The tight packing of cells underneath a bristle limited the ability to isolate the response of single cells. This may contribute to overlap in responses.

Figure legends

Figure 1. *ppk23* and *ppk29* are expressed in gustatory neurons.

A. *ppk23-Gal4* drives expression of *UAS-GFP* in proboscis and *UAS-CD8-GFP* in leg neurons. Shown are the distal three tarsal leg segments for males (m) and females (f). ppk23 is expressed in all legs and additional segments (not shown). Sensory axons labeled with *UAS-GFP* project to the subesophageal ganglion. Scale bar is 40 μm.
B. Two-color *in situ* hybridization with *ppk23* and *ppk29* anti-sense probes demonstrates co-expression in proboscis neurons (top left). In contrast, *ppk23* mRNA is not co-expressed with *Gr64f-Gal4, UAS-CD8-GFP* (top right). *ppk23-Gal4, UAS-CD8-tdTomato* is not co-expressed with *ppk28-lexA, lexAop-CD2-GFP* (bottom left) or the majority of *Gr66a-IRES-GFP* cells (bottom right). Scale bar is 20 μm. See Figure S1 for additional *in situ* hybridizations.

Figure 2. *ppk23-Gal4* is expressed in sexually dimorphic Fru^{M}-positive neurons.

A. Thoracic ganglia from *ppk23-Gal4, UAS-CD8-GFP* males (m) and females (f), showing axon crossing in the prothoracic ganglia of males but not females. Magenta counterstain is nc82 antisera.
B. Male forelegs with fru^{P1}*-LexA, lexAop-CD2-GFP* and *ppk23-Gal4, UAS-CD8-tdTomato* reveal cellular co-expression.
C. Male forelegs co-labeled with *ppk23-Gal4* or fru^{P1}*-LexA* and *ppk28-LexA, Gr32a-Ires-GFP, Gr32a-Gal4, Gr68a-Gal4, Gr64f-Gal4* or *Gr66a-Gal4*. Distal three tarsal segments are shown in all panels, except for fru^{P1}*-LexA, Gr68a-Gal4* in which the most distal segment is not shown, as it lacks *Gr68a-Gal4*. Scale bar is 50 μm. See Figure S2 for proboscis expression of fru^{P1}*-LexA*.

Figure 3. Δ*ppk23* and Δ*ppk29* show courtship defects.

A. Control, Δ*ppk23,* Δ*ppk29* double and single mutants and rescue males were paired with *Canton-S* males and courtship behavior was assayed as number of unilateral wing extensions in a 20-minute trial. Δ*ppk23,* Δ*ppk29* double mutants and Δ*ppk23* mutants increased male-male courtship. The Δ*ppk23* phenotype was rescued by reintroduction of *ppk23* (+*ppk23*) or by removal of the antennae (-ant.) but not by reintroduction of ppk29 (+*ppk29*) into the Δ*ppk23* background. Mean+/-SEM, n=15-26 trials/genotype, except Δ*ppk23* mutants –ant. (n=8). ***P<0.001 compared to control (Kruskal-Wallis test, Dunn's post-hoc).
B. 6-9 males were introduced for 10-minute trials and the fraction of time that males followed each other in chains of 3 or more was measured as the Chaining Index. The Δ*ppk23* phenotype was rescued by reintroduction of *ppk23* (+*ppk23*) or by antennal removal (-ant.) but not by ppk29 (+*ppk29*). Mean+/-SEM, n=6-11 trials/genotype. **P<0.01; ***P<0.001 compared to control (Kruskal-Wallis test, Dunn's post-hoc).
C-D. Control, mutant and rescue males were paired with *Canton-S* females for 30 minute trials and courtship behavior was assayed as number of unilateral wing extensions/min pre-copulation (C) and latency to begin courting (D). Because courtship terminates at copulation and concludes

at different times in the male-female assay, number of wing extensions was divided by the time until copulation. Δ*ppk23* and Δ*ppk29* showed significantly decreased courtship. Defects were rescued by re-introduction of *ppk23* (+*ppk23*) but not ppk29 (+*ppk29*) into Δ*ppk23* or re-introduction of *ppk29* (+*ppk29*) but not ppk23 (+*ppk23*) into the Δ*ppk29* using *ppk23-Gal4*. Mean+/-SEM, n=36-44 trials/genotype for isogenic controls and mutants, n=16-23 for rescue flies. *P<0.05; **P<0.01; ***P<0.001 compared to control (Kruskal-Wallis test, Dunn's post-hoc). See Figure S3 for proboscis extension assays.

Figure 4. Silencing or activating *ppk23* neurons affects courtship behavior to males and females.

A. Whereas control flies do not court males in 20 minute trials, *ppk23-Gal4, UAS-TNT* flies show increased single wing extensions similar to Δ*ppk23* males (shown for comparison, see Figure 3). Inhibiting expression of *UAS-TNT* in *ppk23-Gal4* neurons containing fru^{P1}*-LexA, lexAop-Gal80* blocked wing extensions, whereas inhibiting *UAS-TNT* expression in *ppk23-Gal4, Gr66a-LexA, lexAop-Gal80* cells had no effect. This argues that the Fru^{M}-positive, Ppk23-positive leg neurons mediate inhibition. Red bars denote responses significantly different than *ppk23-Gal4* control. Mean+/-SEM, n=8-21 trials/genotype. ***P<0.001 (Kruskal-Wallis test, Dunn's post-hoc).
B. *ppk23-Gal4, UAS-TNT* males as well as *ppk23-Gal4, UAS-TNT* males with Gr66a cells not silenced (*Gr66a-LexA, lexAop-Gal80*) showed increased courtship latencies toward females in 30 minute trials, similar to *ppk23* mutants. Flies in which TNT is not expressed in Fru^{M}-positive, Ppk23-positive cells (*ppk23-Gal4,UAS-TNT,* fru^{P1}*-LexA, lexAop-Gal80* flies) show normal courtship latency. Red bars denote responses significantly different than *ppk23-Gal4*. Mean+/-SEM, n=21-36 trials/genotype. *P<0.05; **P<0.01 (Kruskal-Wallis test, Dunn's post-hoc).
C. Ppk23 cells were activated by heat-induced depolarization of dTRPA1 and effects on courtship toward oe- males and females were examined in 20 minute trials. Upon activation of dTRPA1 at 30°C, *ppk23-Gal4, UAS-dTRPA1* flies showed decreased male-male courtship and increased male-female courtship compared to controls. Mean+/-SEM, n=15-21 trials/genotype. **P<0.01; ***P<0.001 (ANOVA, square root transformation, TukeyHSD post-hoc).
D. Ppk23 cells were activated by heat-induced depolarization of dTRPA1 and effects on courtship toward oe+ males and females were examined in 20 minute trials. Upon activation of dTRPA1 at 30°C, *ppk23-Gal4, UAS-dTRPA1* flies showed no male-male courtship and increased male-female courtship compared to controls. Mean+/-SEM, n=10 trials/genotype. ***P<0.001 (ANOVA, square root transformation, TukeyHSD post-hoc). See Figure S4 for additional courtship measurements.

Figure 5. Δ*ppk23* and Δ*ppk29* flies do not show behavioral responses to pheromones.

A. Males were placed with oe- males either unpainted or painted with the pheromones 7T, 7P or cVA. These compounds inhibited male-male courtship in controls but had no effect on Δ*ppk23* or Δ*ppk29* behavior. Animals lacking antennae (-ant.) showed reduced male-male courtship.

Mean+/-SEM, n=16-50 trials/genotype/compound. **P<0.01 (Mann-Whitney test to same genotype, no pheromone).
B. Males were placed with oe- females either unpainted or painted with 7,11-HD (HD), 7,11-ND (ND) or 7P. These compounds increased wing extensions toward oe- females by controls but not Δ*ppk23* or Δ*ppk29*, with the exception of 7P for Δ*ppk29*. Mean+/-SEM, n=16-48 trials/genotype. *P<0.05; **P<0.01 (Mann-Whitney test to same genotype, no pheromone). Also, Mann-Whitney test, control vs Δ*ppk23* or Δ*ppk29*, no pheromone = ***P<0.0001.

Figure 6. *ppk23* cells respond to pheromones.

A. A mix of 7,11-HD, 7,11-ND, 7P, 7T and cVA was dissolved in 10% EtOH and applied to single *ppk23-Gal4, UAS-GCaMP3* leg bristles. Mean+/-SEM, n=4-15 cells/sex. *P<0.05; **P<0.01; ***P<0.001 (t-test to 10% EtOH control).
B. *ppk23-Gal4, UAS-GCaMP3* leg cells were stimulated with 1M sucrose, 1M NaCl and 1mM quinine. Mean+/-SEM, n=6-15 cells/sex. *P<0.05 (t-test to EtOH control).
C-D. Responses from *ppk23-Gal4, UAS-GCaMP3* cells in wildtype, Δ*ppk23*, Δ*ppk23* + *ppk23*, and Δ*ppk29* backgrounds were monitored upon single bristle stimulation with 10% EtOH for reference or a mix of 7,11-HD, 7,11-ND, 7P, 7T and cVA dissolved in 10% EtOH. *ppk23* cells from male and female legs (C) or from male and female proboscis (D) were assayed. Mean+/-SEM, n=3-9 cells/sex. *P<0.05; **P<0.01; ***P<0.001 (t-test to *ppk23* mutant).
E. Misexpression of *ppk23* and *ppk29* in *ppk28* cells in a Δ*ppk28* background failed to confer responses to the pheromone mix. 10% EtOH or 100ng pheromone mix in 10% EtOH were used for stimulation. Fly genotype for misexpression is Δ*ppk28, UAS-ppk29; UAS-G-CaMP3, UAS-ppk23; ppk28-Gal4*. Mean+/-SEM, n=8-14 cells/genotype. (t-test to EtOH controls; ns).

Figure 7: *ppk23* cells selectively respond to male or female pheromones.

A. Sample responses of two *ppk23* cells underneath a chemosensory bristle on the leg (M4 in C). First image is pseudocolor baseline fluorescence. Other images are ΔF/F for the compounds listed. Outlined are the positions of the two cells. Scale bar is 10μm.
B. Classifying the two cells under one bristle as "female" or "male" based on maximum response shows a bimodal distribution in which cells that respond to 7,11-HD or 7,11-ND do not respond to 7P or 7T and respond less to cVA. Mean+/-SEM, n=8 bristles, 2 cells/bristle. *P<0.05; **P<0.01; ***P<0.001 (t-test to 10% hexane control).
C. Responses of individual cells are color-coded as %ΔF/F relative to maximum ΔF/F of the cell. Four chemosensory bristles from males (M1-M4) or females (F5-F8) were stimulated and the two cells under a bristle were categorized as "female" or "male" based on response profiles. Each bristle has one cell that responds best to female compounds and another cell that responds best to male compounds. The tight packing of cells may contribute to overlap in responses.

Figure 8. Calcium imaging reveals that *ppk25* cells respond specifically to female pheromones.

A. Solutions (100 ng/μl in 10%hexane, 90% water) of 7,11-HD (HD), 7,11-ND (ND), 7T, cVA, a mixture of all pheromones (mix) or 10% hexane, 90% water solution alone (hex) were applied

to single leg bristles of *ppk25-Gal4, 20×UAS-GCaMP3* flies. "*wt*" flies contained one copy of the normal *ppk25* gene. *ppk25 null* mutants were heterozygous for two different deletions of the *ppk25* locus, and "*ppk25* rescue" flies are *ppk25*mutants carrying *UAS-ppk25* and *ppk25-Gal4* transgenes to target *ppk25* expression to *ppk25* cells . "#" denotes pheromones that did not elicit responses significantly higher than hexane alone in "*wt*" flies and were not tested further. n = 7–10; Mean ± SEM; ttest to *wt*, *p<0.05, **p<0.01.

B. The same pheromone solutions as in A were applied to single leg bristles of *ppk25* mutants carrying the *ppk23-Gal4* and *20×UAS-GCaMP3* transgenes. As previously observed in flies with normal *ppk25* genes, one population of *ppk23* cells, the M cells, respond specifically to male pheromones. In contrast to *wt* males however, in *ppk25 null* mutants the second population of *ppk23*cells, corresponding to F cells does not respond to any pheromone. n = 8; Mean ± SEM; ttest to *wt*,*p<0.05,**p<0.01.

Figure 1.

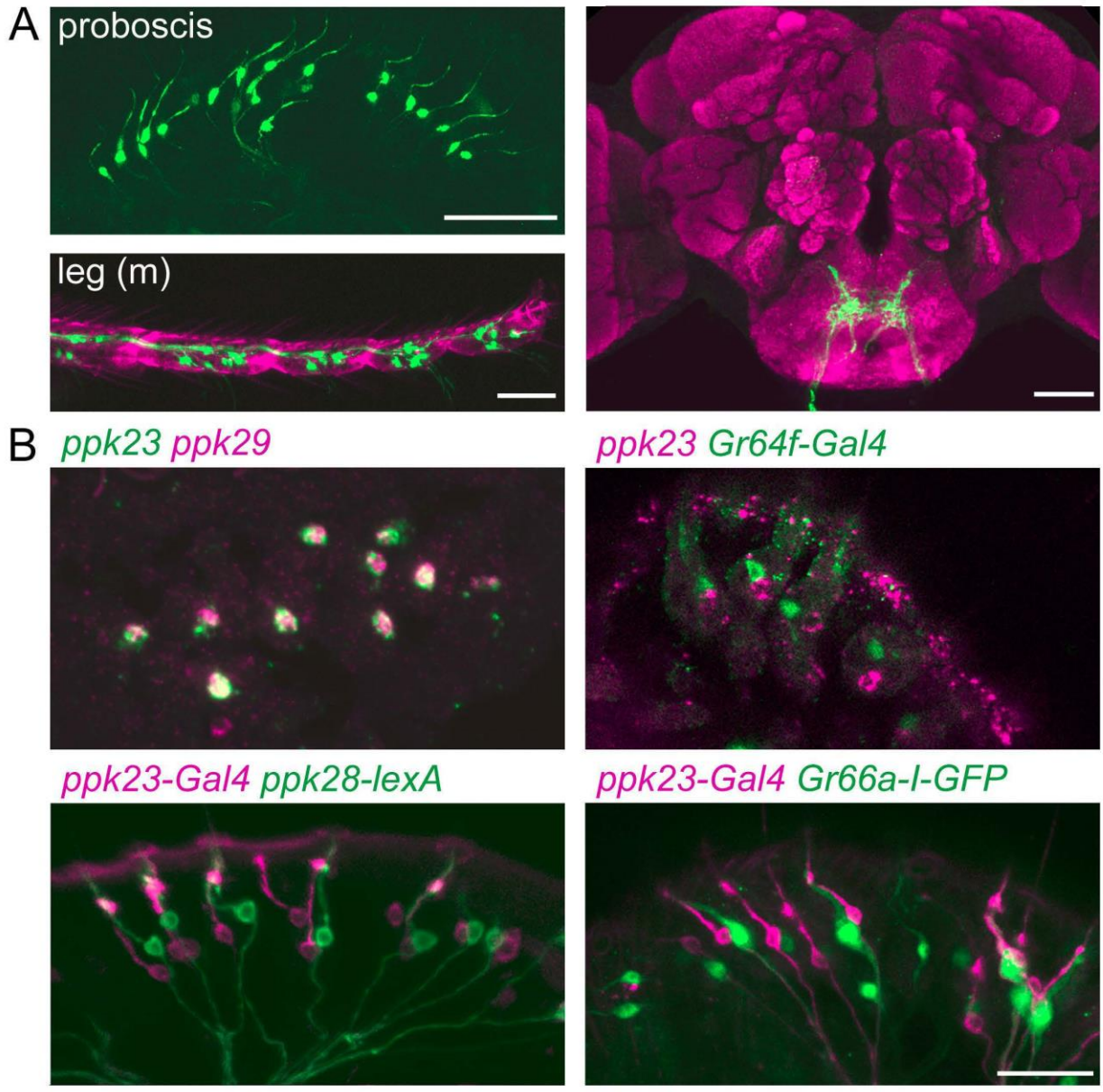
A
proboscis
leg (m)
B
ppk23 ppk29
ppk23 Gr64f-Gal4
ppk23-Gal4 ppk28-lexA
ppk23-Gal4 Gr66a-I-GFP

Figure 2.

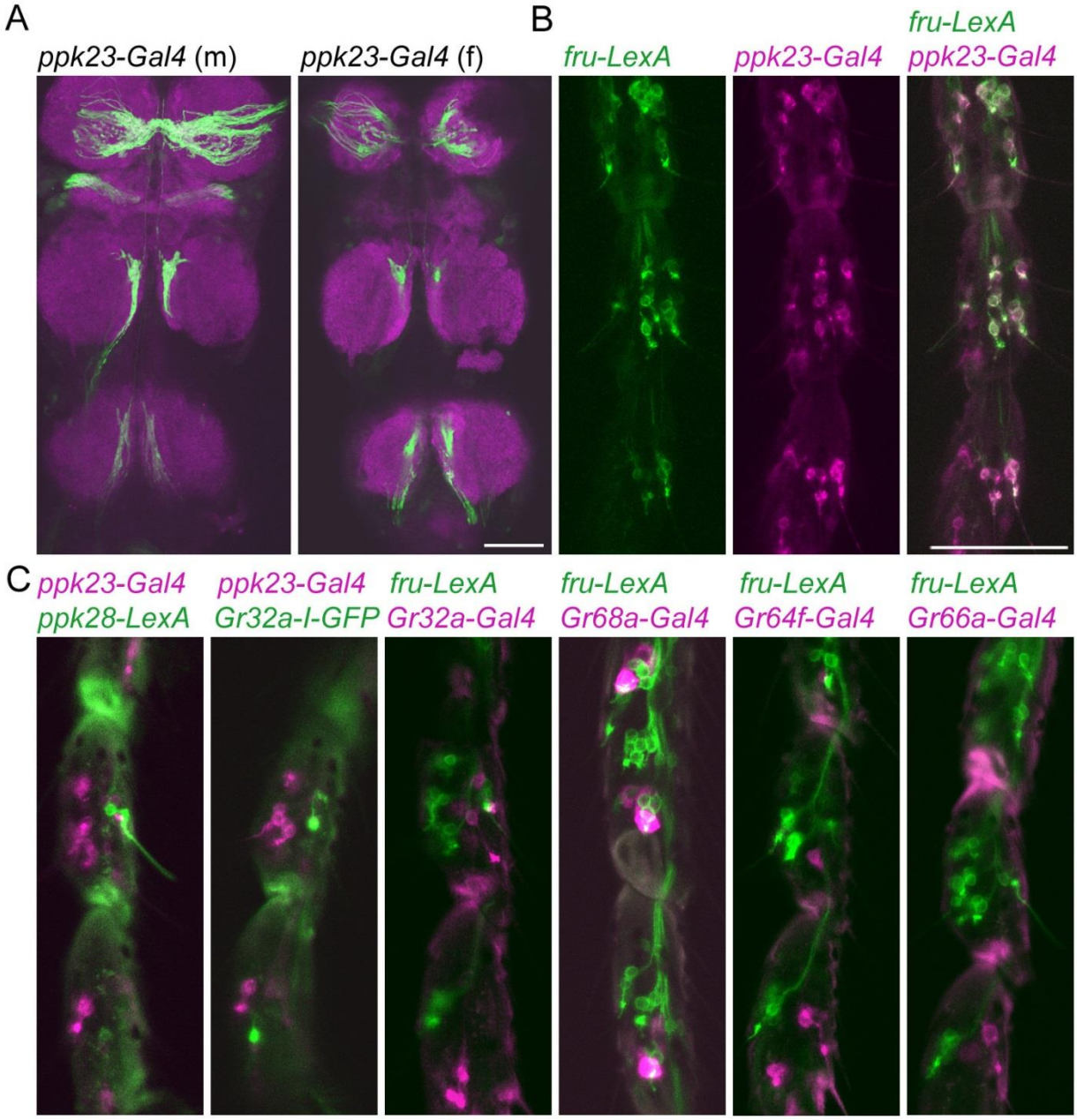
A
ppk23-Gal4 (m)
ppk23-Gal4 (f)
B
fru-LexA
ppk23-Gal4
fru-LexA
ppk23-Gal4
C
ppk23-Gal4
ppk28-LexA
ppk23-Gal4
Gr32a-I-GFP
fru-LexA
Gr32a-Gal4
fru-LexA
Gr68a-Gal4
fru-LexA
Gr64f-Gal4
fru-LexA
Gr66a-Gal4

Figure 3.

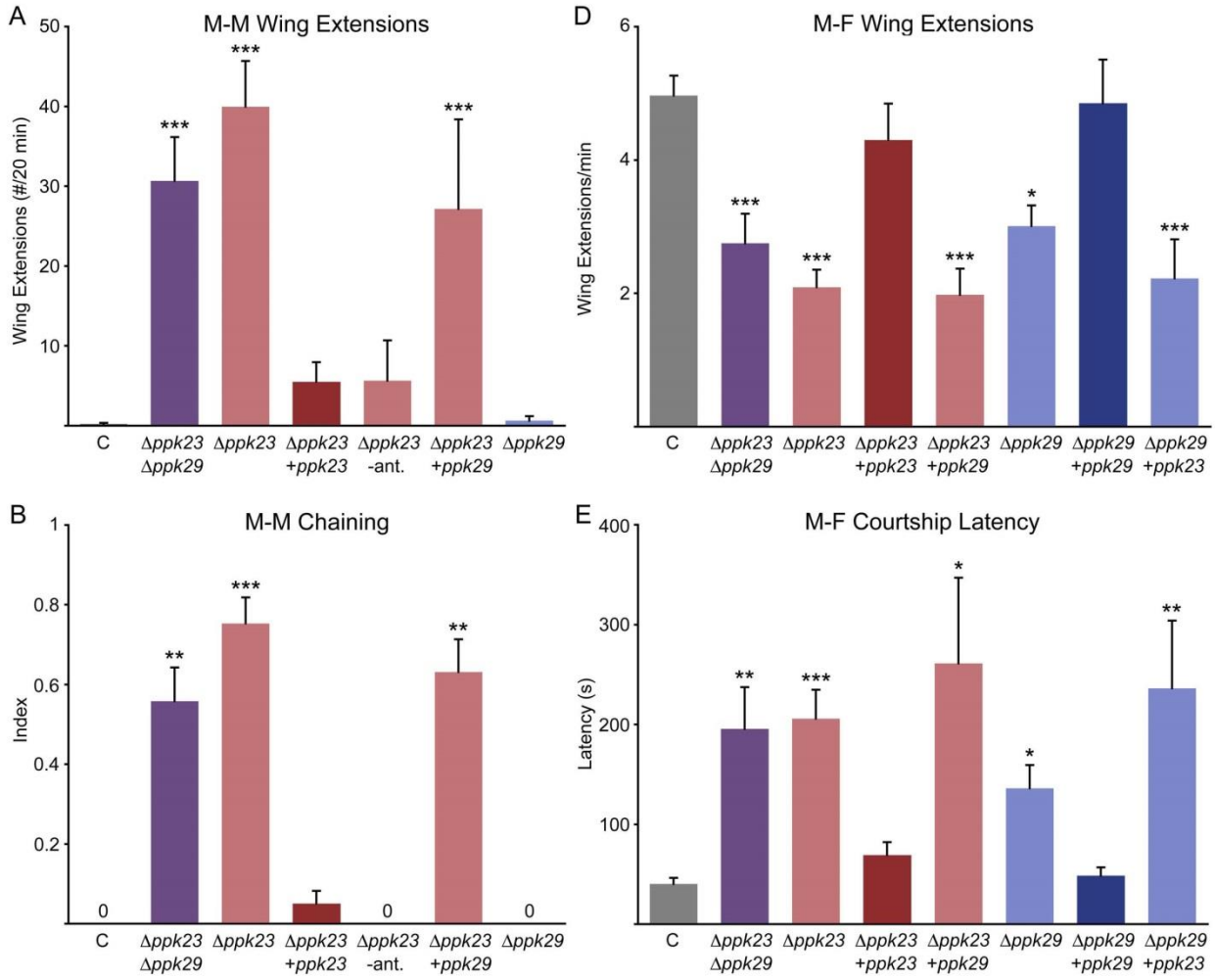
A
M-M Wing Extensions
Wing Extensions (#/20 min)
50
40
30
20
10
***
***
***
C
Δppk23 Δppk29
Δppk23
Δppk23 +ppk23
Δppk23 -ant.
Δppk23 +ppk29
Δppk29
D
M-F Wing Extensions
Wing Extensions/min
6
4
2
***
***
***
*
***
C
Δppk23 Δppk29
Δppk23
Δppk23 +ppk23
Δppk23 +ppk29
Δppk29
Δppk29 +ppk29
Δppk29 +ppk23
B
M-M Chaining
Index
1
0.8
0.6
0.4
0.2
0
**
***
**
0
0
C
Δppk23 Δppk29
Δppk23
Δppk23 +ppk23
Δppk23 -ant.
Δppk23 +ppk29
Δppk29
E
M-F Courtship Latency
Latency (s)
400
300
200
100
**
***
*
*
**
C
Δppk23 Δppk29
Δppk23
Δppk23 +ppk23
Δppk23 +ppk29
Δppk29
Δppk29 +ppk29
Δppk29 +ppk23

Figure 4.

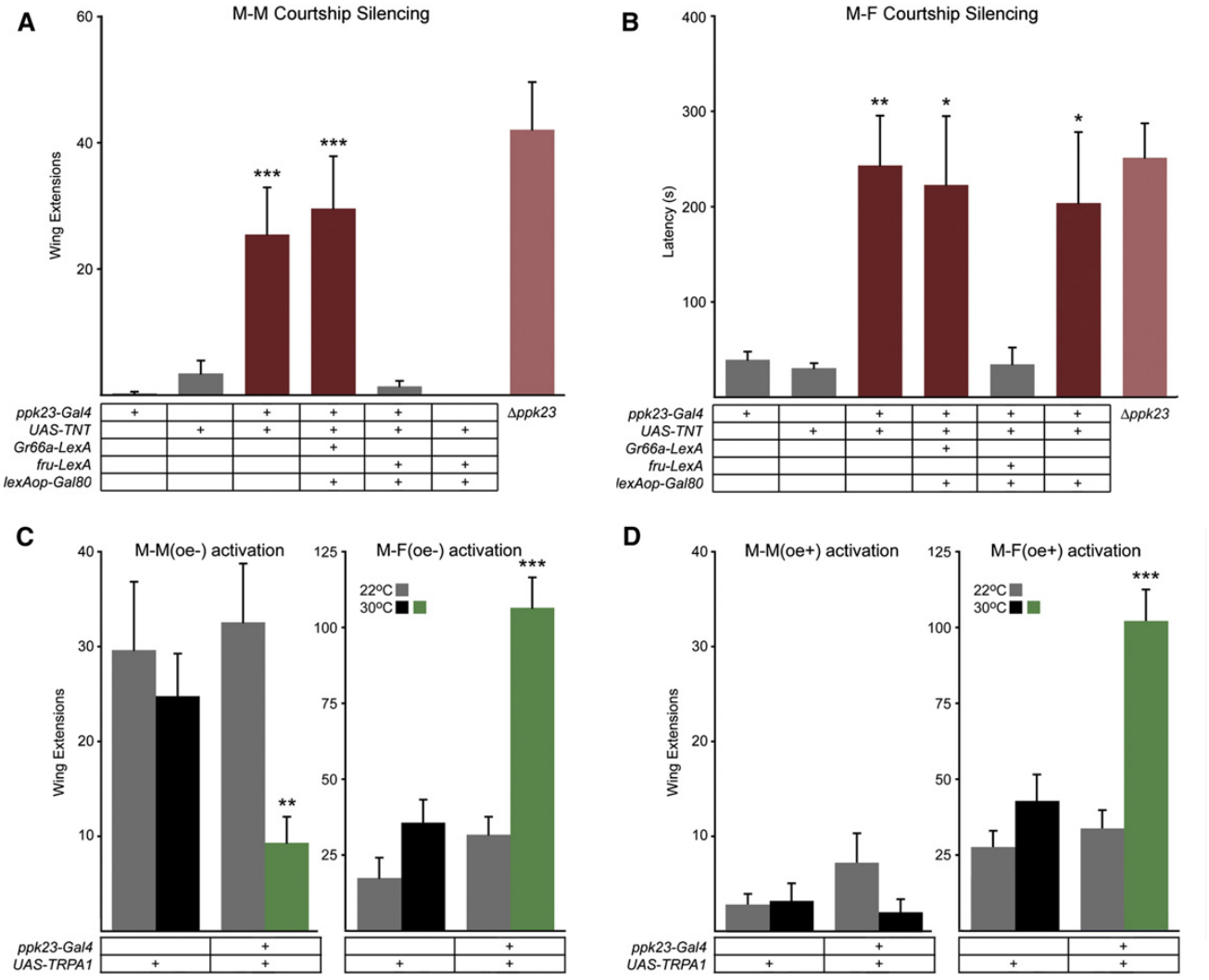
A
M-M Courtship Silencing
Wing Extensions
60
40
20
***
***
ppk23-Gal4
UAS-TNT
Gr66a-LexA
fru-LexA
lexAop-Gal80
Δppk23
B
M-F Courtship Silencing
Latency (s)
400
300
200
100
**
*
*
ppk23-Gal4
UAS-TNT
Gr66a-LexA
fru-LexA
lexAop-Gal80
Δppk23
C
M-M(oe-) activation
M-F(oe-) activation
Wing Extensions
40
30
20
10
125
100
75
50
25
22ºC
30ºC
**
***
ppk23-Gal4
UAS-TRPA1
D
M-M(oe+) activation
M-F(oe+) activation
Wing Extensions
22ºC
30ºC
***
ppk23-Gal4
UAS-TRPA1

Figure 5.

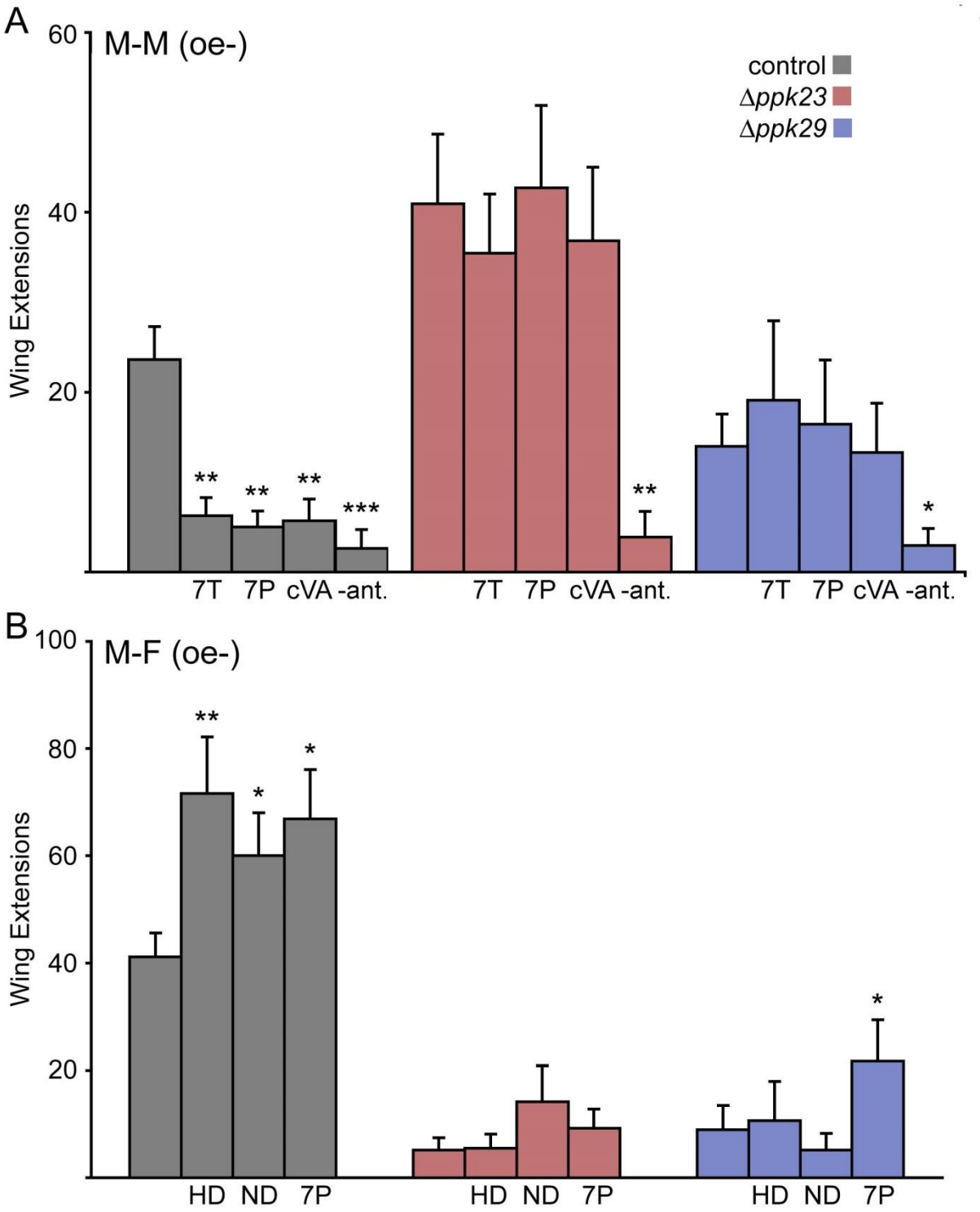
A
M-M (oe-)
control
Δppk23
Δppk29
Wing Extensions
60
40
20
**
**
**
***
**
*
7T
7P
cVA
-ant.
7T
7P
cVA
-ant.
7T
7P
cVA
-ant.
B
M-F (oe-)
Wing Extensions
100
80
60
40
20
**
*
*
*
HD
ND
7P
HD
ND
7P
HD
ND
7P

Figure 6.

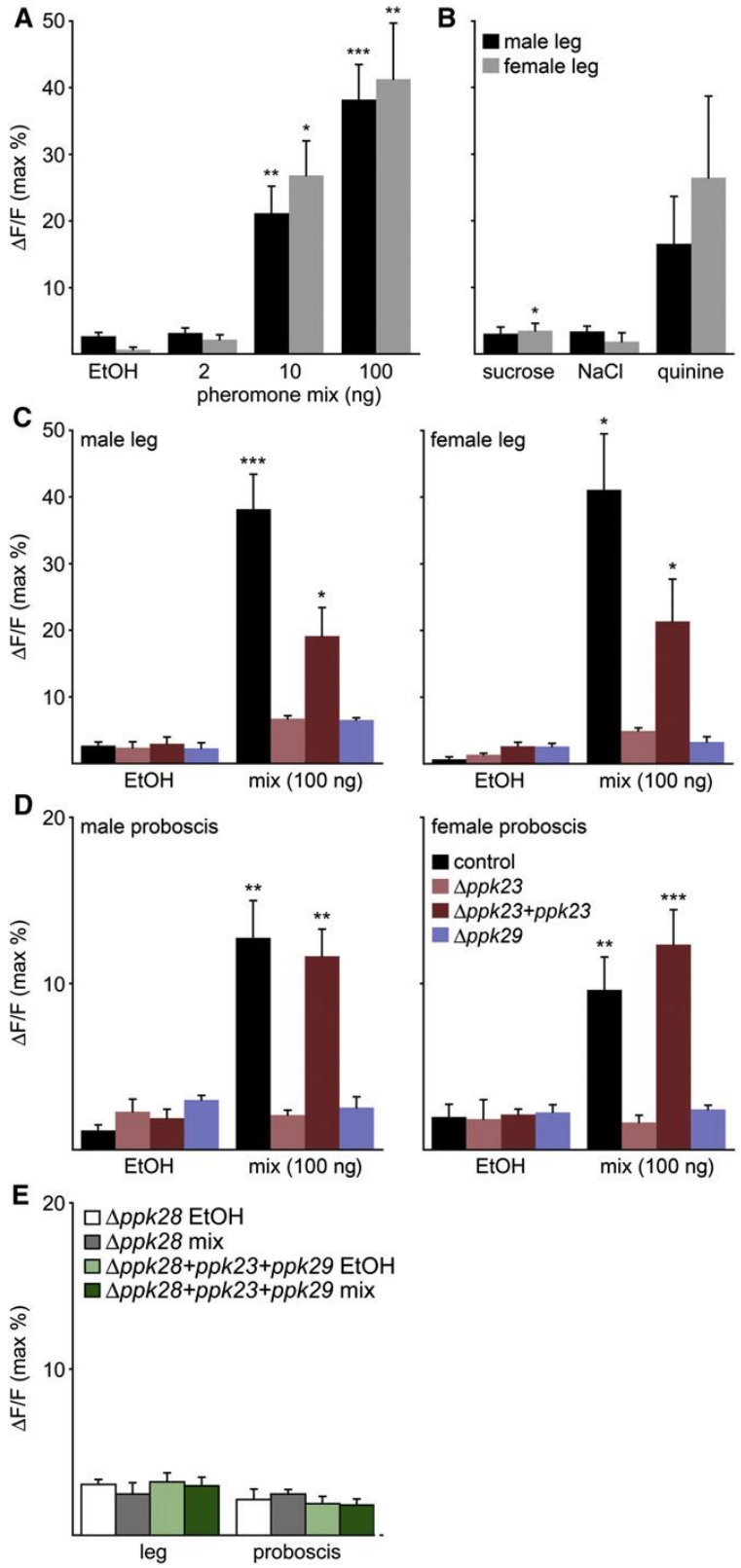
A
ΔF/F (max %)
EtOH
2
10
100
pheromone mix (ng)
B
male leg
female leg
sucrose
NaCl
quinine
C
male leg
female leg
EtOH
mix (100 ng)
D
male proboscis
female proboscis
control
Δppk23
Δppk23+ppk23
Δppk29
E
Δppk28 EtOH
Δppk28 mix
Δppk28+ppk23+ppk29 EtOH
Δppk28+ppk23+ppk29 mix
leg
proboscis

Figure 7.

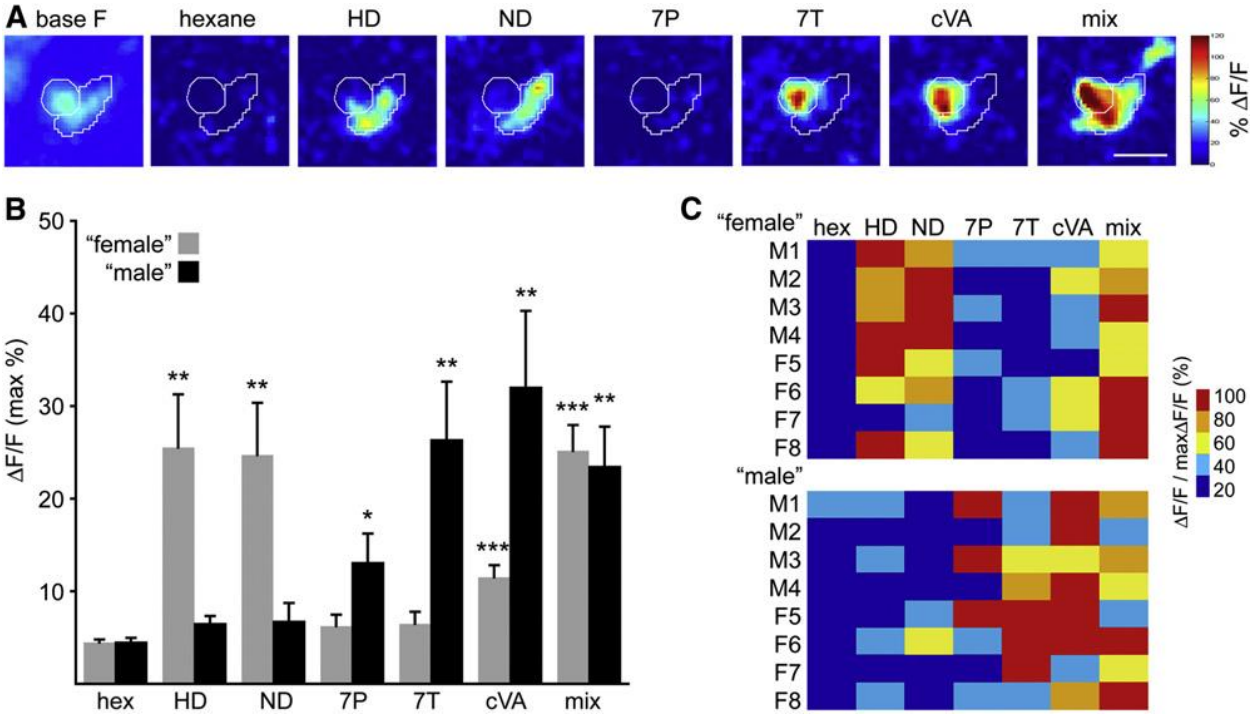
A
base F
hexane
HD
ND
7P
7T
cVA
mix
% ΔF/F
B
"female"
"male"
ΔF/F (max %)
hex
HD
ND
7P
7T
cVA
mix
C
"female"
"male"
M1
M2
M3
M4
F5
F6
F7
F8
ΔF/F / maxΔF/F (%)

Figure 8.

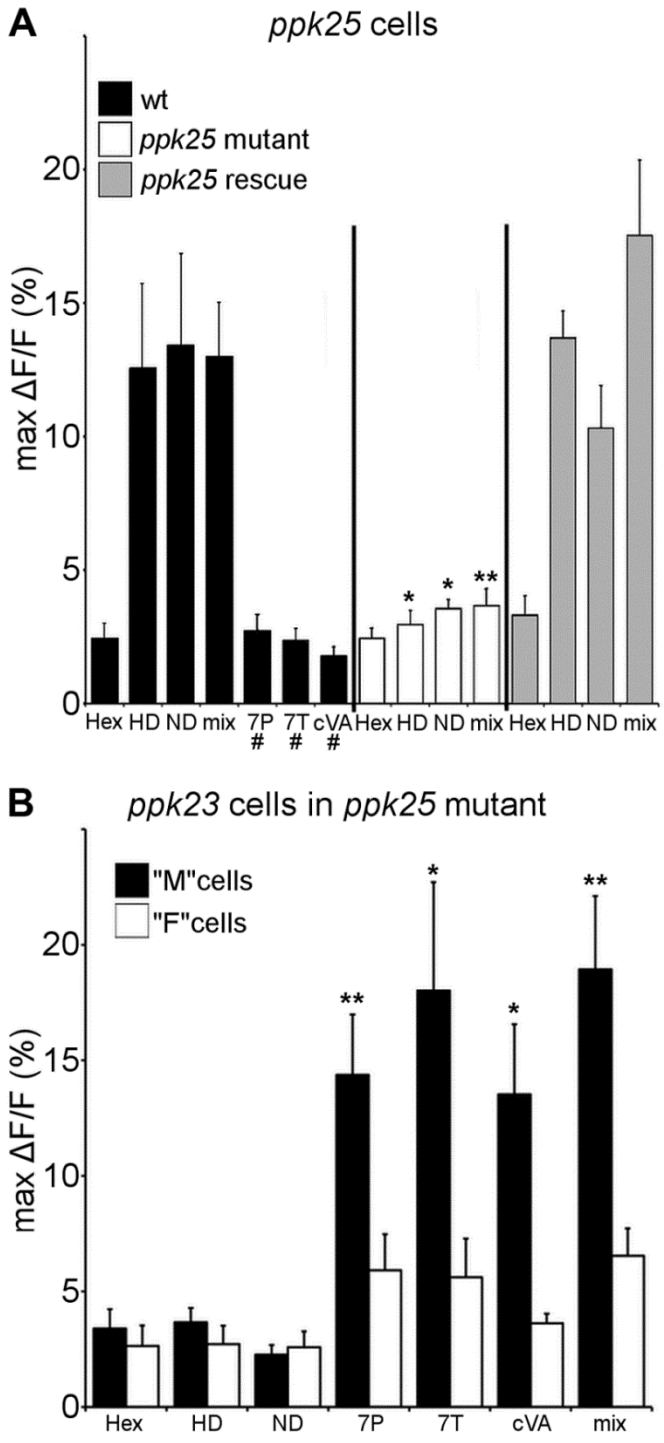
A
ppk25 cells
wt
ppk25 mutant
ppk25 rescue
max ΔF/F (%)
0
5
10
15
20
Hex HD ND mix 7P # 7T # cVA # Hex HD ND mix Hex HD ND mix
*
*
**
B
ppk23 cells in ppk25 mutant
"M"cells
"F"cells
max ΔF/F (%)
0
5
10
15
20
Hex HD ND 7P 7T cVA mix
**
*
*
**

Supplemental Figure legends

Figure S1: Expression studies of *ppk23* and *ppk29*, related to Figure 1.

A. *ppk29-Gal4* drives expression of *UAS-CD8-GFP* in proboscis and leg neurons of both sexes. A leg from a male (m) is shown. Sensory axons project to the subesophageal ganglion in the brain. The axon projection signal is faint, resulting in high green background in the brain.

B. *ppk23* anti-sense DIG probe is co-expressed with *ppk23-Gal4, UAS-GFP* in proboscis neurons. (84/93 [90.3%] *ppk23-Gal4* neurons expressed *ppk23*, 84/84 [100%] *ppk23*-expressing neurons expressed *ppk23-Gal4*$_{2.1}$).

C. *ppk11-Gal4, UAS-CD2* is expressed in support cells based on morphology and lack of axonal projections, whereas *Gr22e-I-GFP*, a marker for bitter cells, is expressed in neurons.
D. *ppk23* is not co-expressed with *ppk28* by double in situ hybridization. (0/51 *ppk23* neurons expressed *ppk28). ppk23* DIG probe and *ppk28* FITC probe were used.
Scale bars are 50 μm.

E. *ppk23* is not co-expressed with the majority of *Gr66a* cells by double in situ hybridization (25/84 [29.7%] *ppk23* neurons expressed *Gr66a*). *ppk23* anti-sense DIG probe, *Gr66a* anti-sense FITC probe were used. Scale bars are 40 μm.

Figure S2: FruM expression in the proboscis, related to Figure 2.

A. *fru*^{P1}*-LexA, lexAop-CD2-GFP* is not co-expressed with *ppk23-Gal4*, *ppk28-Gal4*, *Gr5a-Gal4* or *Gr66a-Gal4*, arguing that it is not in *ppk23* cells or water, sugar or bitter cells.

B. *ppk23-Gal4, UAS-CD8-GFP* neurons send dendrites that extend out to the bristle tip, indicative of chemosensory neurons. *fru*^{P1}*-LexA*, *lexAop-CD2-GFP* neurons terminate at the base of the bristle, characteristic of mechanosensory cells. Shown in higher resolution in the bottom panels. Scale bars are 50 μm.

Figure S3: *ppk23, ppk29* mutants respond to taste compounds, related to Figure 3.

Proboscis extension to taste compounds was monitored as in Wang, et al. 2004. Flies, aged 7-14 days, were starved overnight with water, immobilized on coverslips with nail polish, placed in a humidified chamber for 2 hours then monitored for extension to taste compounds delivered to tarsi. Before examining extension, flies were stimulated with water on the tarsi and allowed to drink ad libitum until they did not extend to three consecutive water stimulations. The number of flies that drank water on the first water stimulation was recorded for % PER to H2O. All other compounds were delivered three times followed by water and number of extensions recorded. Assays were conducted on 14-20 flies/genotype/trial, 3 independent trials for two groups of stimuli. Stimuli were delivered in order: Group one, 50mM NaCl, 500mM NaCl plus 50mM sucrose, 100mM sucrose; Group two, bitter, sugar, bitter, sugar, with randomized 1mM

denatonium plus 100mM sucrose or 10mM quinine plus 100mM sucrose for bitter; 50mM sucrose, 100mM glucose for sugar. Mean +/- 95% CI. Fisher's exact test to control, NS.

Figure S4: Male-Female Courtship defects associated with ppk23, related to Figure 4.

A. Control, *ppk23, ppk29* double mutant, single mutant and rescue males were paired with *Canton-S* females and failure to court was assayed. *ppk23, ppk29* double and single mutants showed significantly decreased courtship. These defects were rescued by re-introduction of *ppk23* (+*ppk23*) into the *ppk23* mutant or re-introduction of *ppk29* (+*ppk29*) but not ppk23 (+*ppk23*) into the *ppk29* mutant. Mean +/- 95% CI, n= 36-44 trials/genotype for isogenic controls and mutants, n = 16-23 for rescue flies. *p<0.05; ***p<0.001 compared to control (Fisher's exact test).

B. Males were paired with *Canton-S* females in a 30 minute courtship assay and failure to court was assayed. *ppk23-Gal4, UAS-TNT* males as well as *ppk23-Gal4, UAS-TNT* males with Gr66a cells not silenced (*Gr66a-LexA, lexAop-Gal80*) showed failure to court. This courtship is not statistically different from controls. Mean +/- 95% CI (Fisher's exact test).

C. *ppk23-Gal4, UAS-TNT* males as well as *ppk23-Gal4, UAS-TNT* males with Gr66a cells not silenced (*Gr66a-LexA, lexAop-Gal80*) showed decreased single wing extensions/minute, similar to *ppk23* mutants. Flies in which TNT is not expressed in Fru^{M}-positive, Ppk23-positive cells (*ppk23-Gal4,UAS-TNT, fru^{P1}-LexA, lexAop-Gal80* flies) show normal wing extensions, arguing that these cells promote male-female courtship. Red bars denote responses significantly different than *ppk23-Gal4* control. Mean +/- SEM, n=21-36 trials/genotype. *p<0.05; ***p<0.001 (Kruskal-Wallis test, Dunn's post-hoc).

D. Ppk23 cells were activated by heat-induced depolarization of dTRPA1 and effects on courtship toward oe- males and females, lacking cuticular hydrocarbons, were examined in 20 minute trials. Assays were performed in the dark and antennae were removed from courting males to remove other sensory inputs. No flies courted under these conditions. Mean+/-SEM, n=9-10trials/genotype. (ANOVA, square root transformation, TukeyHSD post-hoc, ns).

Supplemental Figure 1.

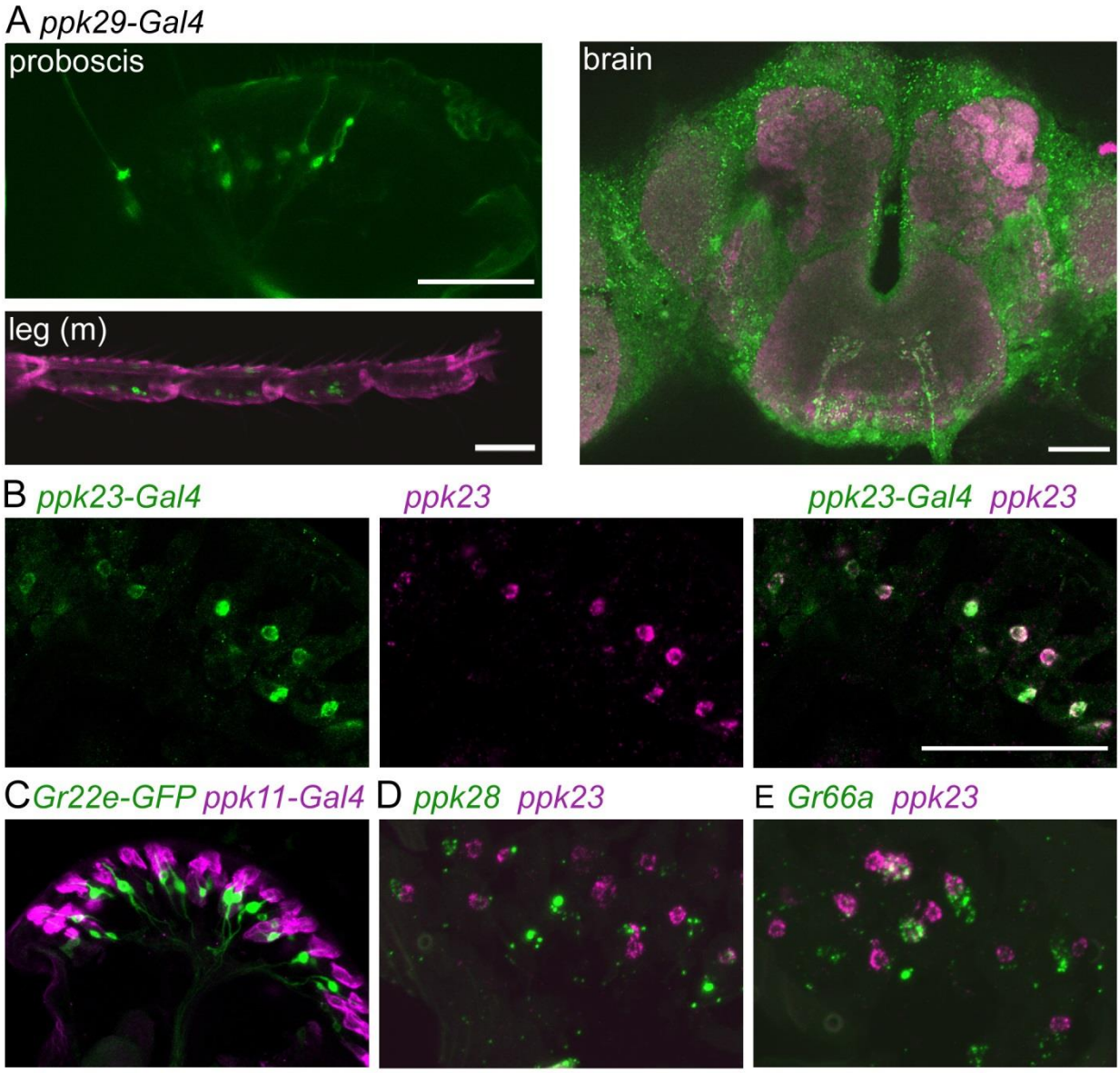

Supplemental Figure 2.

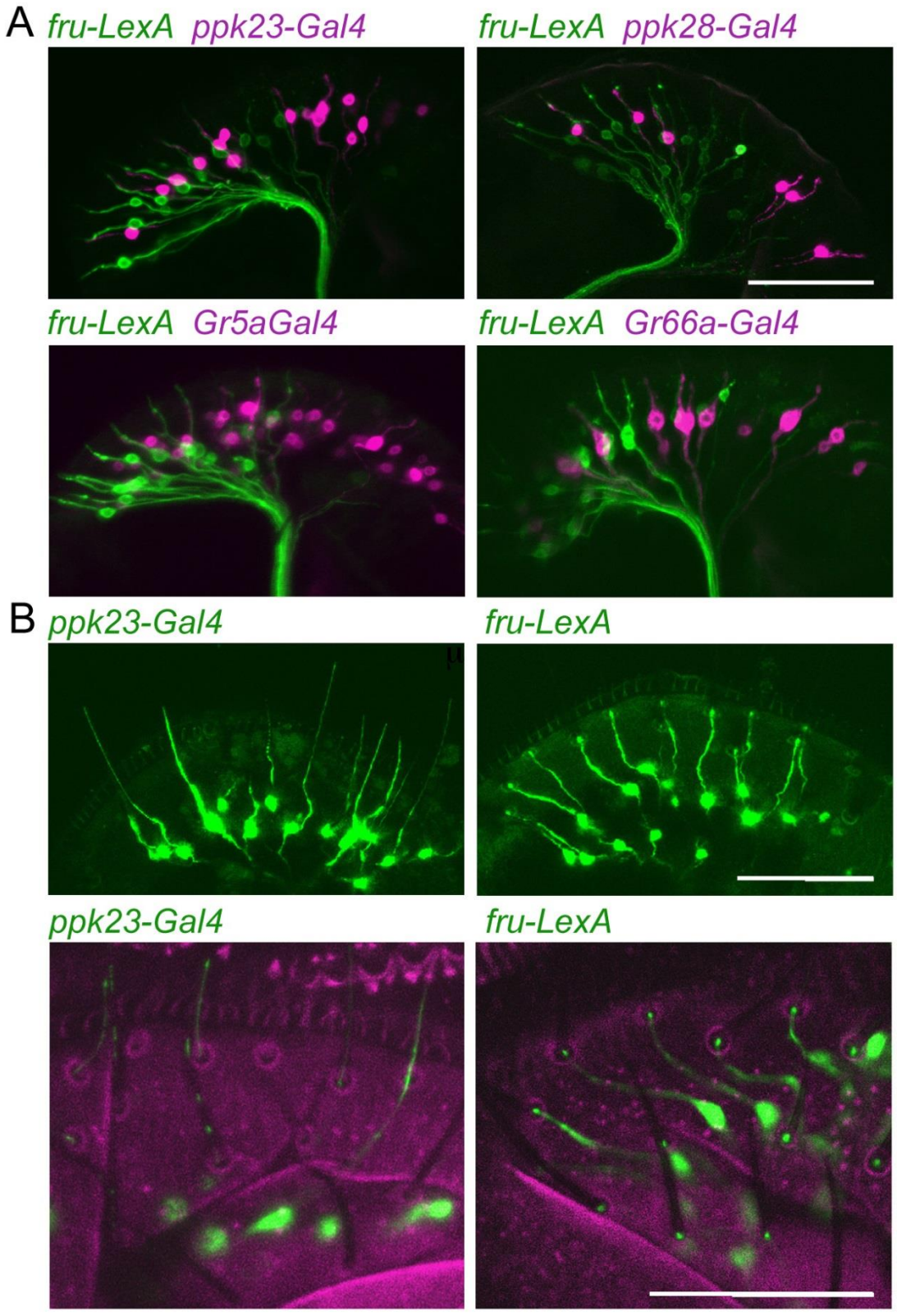

Supplemental Figure 3.

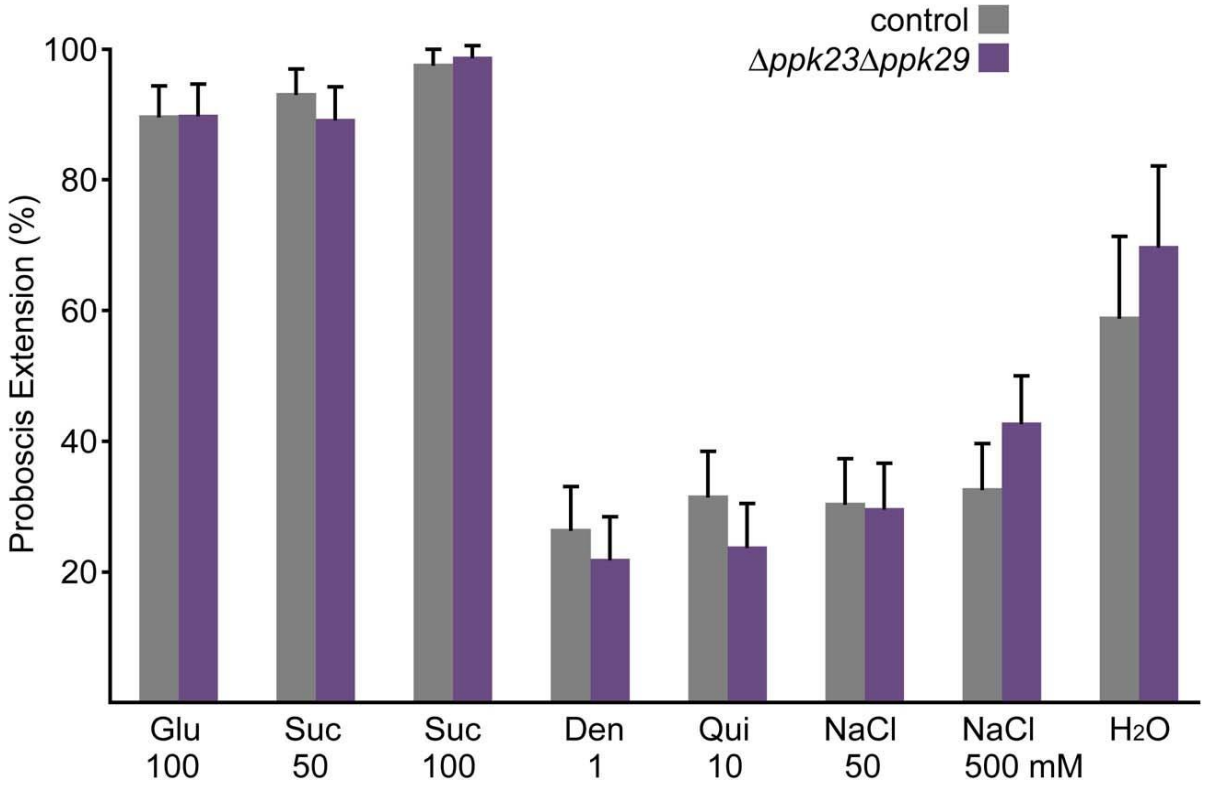

Supplemental Figure 4.

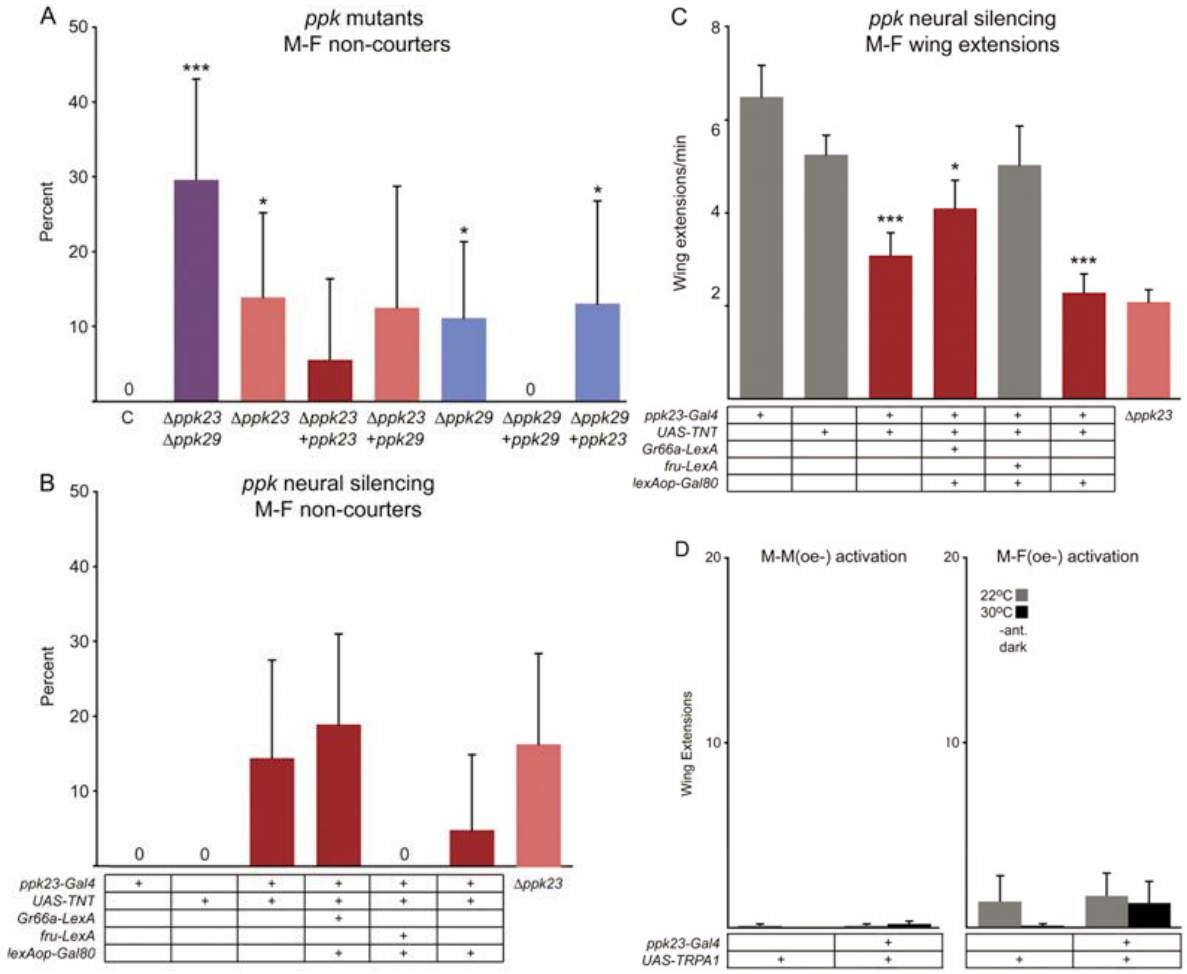

Chapter 3:

The PPK28 osmosensitive ion channel is directly gated by mechanical force

Preceding Remarks

In this chapter we utilize pharmacological and electrophysiological approaches to examine how pickpocket ion channels may be gated. These data are unpublished but have been formatted into a manuscript which is reproduced below. I performed the experiments including calcium imaging, electrophysiology, and fly behavior. Diana Bautista and Kristin Scott co-supervised the project and co-wrote the manuscript.

Summary

Mechanosensation and osmosensation underly touch, hearing, and body-fluid homeostasis but few mechanosensitive ion channels have been identified. Members of the Degenerin/Epithelial Sodium Channel (Deg/ENaC) family have been implicated in mechanosensation and osmosensation but have not been shown to be direct sensors of mechanical force. A *Drosophila* member of this family, PPK28, mediates water taste detection and confers osmosensitivity to heterologous cells, suggesting that it may sense osmolarity-induced changes in membrane tension. Here, we show that cells misexpressing PPK28 respond to radial stretch, molecules that insert into the membrane outer leaflet, and negative pressure and these responses are inhibited by the Deg/ENaC channel blocker, amiloride. Moreover, a mutation in the selectivity filter of the channel alters the conductance of pressure-evoked currents and placing the cytoplasmic domains of PPK28 onto another PPK member confers pressure sensitivity. This work demonstrates that PPK28 is a mechanically activated channel and provides a molecular platform to study the basis of mechanosensing by the Deg/ENaC channel family.

Introduction

Detection of water is integral for an organism's survival. In order to regulate osmotic homeostasis via water intake, the organism must be able to discriminate between water sources that vary in solute concentration. Water tonicity detection occurs at the level of sensory neurons that monitor either environmental or internal concentrations of solutes. Mammalian central osmosensation has been studied most extensively in the sensory cirumventricular organs of the brain. Recordings in hypothalamic slices have demonstrated that hyperosmotic solutions depolarize magnocellular neurosecretory cells through activation of nonselective cation currents. Misexpression experiments implicate the transient receptor potential channel TRPV4 as a molecular sensor for water because its expression confers sensitivity to hypotonic solutions. However, behavioral support for this model in genetic knock-out animals remains controversial. A related TRP channel in *C. elegans,* OSM-9, has also been shown to function as an osmosensor for hypertonic solutions and mediates escape response behavior. Despite these studies, our understanding of the molecules that detect water and their biophysical properties is limited.

Drosophila utilize gustatory sensory neurons to sample their chemical environment when making consumption decisions. The gustatory system in flies is segregated in the periphery such that dedicated sets of sensory neurons mediate the detection of certain taste classes: sugars, bitter compounds, pheromone molecules, and water. Detection of these modalities is accomplished at the molecular level either through gustatory receptor proteins or through ion channels. Previous work uncovered the ion channel PPK28 as the molecular sensor for water in the fly periphery. Its expression is required for water drinking behavior as well as the neural response to water exposure. Moreover, misexpression of this channel in water-insensitive neurons or in heterologous cells renders them osmotically sensitive. Although much work has been done characterizing the neural substrate for water detection, the mechanism of molecular participation of the Ppk28 ion channel remains unknown.

Here we explore the mechanism of gating of PPK28 using multiple cellular membrane manipulations. Calcium responses are seen in *ppk28* expressing cells after exposure to low osmotic solution, radial stretch, and membrane deformation using crenator molecules. In addition, non-selective cationic currents are carried by PPK28 channels under high speed pressure-clamped electrophysiology. These currents are inhibited in the presence of amiloride, a known ENaC blocker. Finally, water-independent membrane expansion is sufficient to activate water responsive neurons and drive drinking behavior *in vivo*, demonstrating that PPK28 channels function by monitoring local changes at the cellular membrane.

Results

We previously showed that HEK293T cells that express PPK28 respond to low osmolarity by Fluo-4 calcium imaging (Cameron, P. et al., 2010). We confirmed that this response is mediated by Deg/ENaC channel function, as it was inhibited by the Deg/ENaC blocker, amiloride, but not by other channel blockers (Fig. 1). In addition, the response required extracellular calcium, suggesting that PPK28 is a non-selective cation channel (Fig. 1). To test the hypothesis that PPK28 senses low osmolarity by detecting changes in membrane tension, we tested whether membrane deformation could activate PPK28 cells. Cells expressing *ppk28* were seeded on silicone membranes and negative pressure pulses were applied to the membrane to generate radial stretch (Bhattacharya, MRC et al., 2008). Increasing radial stretch from 5-25% caused calcium transients in PPK28 cells, with responses proportional to stretch intensity (Fig. 1). Radial stretch-induced responses were blocked by amiloride (Fig. 1d), arguing that they are mediated by a Deg/ENaC channel. Transfection of a related *Drosophila* gene, *ppk23*, (Thistle, R. et al., 2012) did not generate stretch-evoked calcium responses (Fig. 1d) and transfection of *ppk28* into two additional cell lines also conferred stretch sensitivity (Fig. 1e), arguing for the specificity of the PPK28 response. Together, these data demonstrate that PPK28 confers stretch sensitivity as well as osmosensitivity to heterologous cells.

To examine whether PPK28 detects mechanical deformation at the cell membrane, we applied chemicals that insert into the membrane leaflet. Trinitrophenol (TNP) is an amphipathic molecule that preferentially inserts into the outer leaflet, causing convex deformation of the cell membrane, whereas chlorpromazine (CPZ) inserts into the inner leaflet, causing concave deformation (Fang, J. et al., 2007). Isotonic solutions containing TNP evoked dose-sensitive calcium responses in HEK293T cells expressing *ppk28* whereas CPZ had no effect (Fig. 2a-c). These data suggest that PPK28 detects membrane swelling, consistent with its physiological role in reporting low osmolarity.

Given that TNP activated PPK28 cells in a heterologous system, we asked whether it might activate PPK28 sensory neurons *in vivo* and contribute to behavior in the fly. We used *ppk28-Gal4, UAS-GCaMP3* flies to monitor calcium responses of PPK28 proboscis taste neurons upon TNP exposure (Thistle, R. et al., 2012). High osmolarity (20% Polyethylene glycol (PEG)) was used to prevent endogenous activation of PPK28 cells by water (Cameron, P. et al., 2010) and strictly test the effect of TNP on sensory neuron activation. While 20% PEG inhibited the response of PPK28 neurons to water, the inclusion of increasing concentrations of TNP activated PPK28 cells (Fig. 2d). This activation required PPK28, as Δ*ppk28* flies failed to respond to TNP and reintroduction of the *ppk28* gene into Δ*ppk28* mutants restored TNP responses. To test whether activation of water taste neurons by TNP could contribute to water taste behavior, we asked whether stimulation of taste neurons with TNP caused proboscis extension to initiate consumption, mimicking the behavior of thirsty flies to water. Desiccated flies showed proboscis extension upon water sensory stimulation, this response was blunted in the presence of 20% PEG, restored upon addition of TNP, and required PPK28 (Fig. 2e). These studies demonstrate that TNP activates PPK28 cells and drives water taste behavior, similar to activation by low osmolarity, and suggest that membrane swelling activates PPK28.

Members of the Deg/ENaC family have previously been shown to be expressed in mechanically sensitive cells and have been proposed to function as mechanically activated

channels (Mano, I., 1999). To test whether PPK28 is directly gated by mechanical force, we monitored currents in PPK28 cells upon rapid application of negative pressure ranging from 0-70mm Hg, using cell-attached recordings. Negative pressure generated currents in PPK28 cells (as well as in MPiezo1 cells) that increased with pressure intensity and were blocked by amiloride (Fig. 3a,b). Responses showed a linear current-voltage relationship with the reversal potential at 0-5mV, consistent with a non-voltage-gated, non-selective cation channel (Fig. 3c). Finally, the current-pressure relationship when fitted with a Boltzmann equation yields a P50 of 42.625 mmHg. These data are consistent with mechanical activation of PPK28.

To test whether pressure-evoked currents are directly carried by PPK28 channels, we introduced a pore mutation predicted to alter ion selectivity. Previous studies identified the G/SxS motif preceding TM2 as the ENaC selectivity filter and showed that replacing the terminal serine with a bulky residue switched ENaC from a sodium-selective to a non-selective channel (Brown, AL. et al., 2007). In sodium-selective ENaC members, the middle x residue is often small, such as alanine or glycine, whereas PPK28 contains a phenylalanine and is non-selective (Brown, AL. et al., 2007; Eastwood, AL., 2012). We therefore hypothesized that converting phenylalanine to alanine would convert PPK28 from a non-selective to a sodium-selective channel. Indeed, cells expressing the PPK28 F499A mutant produced pressure-evoked currents with a reversal potential shifted to the sodium reversal potential (Fig. 4a) and no longer exhibited calcium responses to hypotonic perfusion (Fig. 4b), demonstrating that altering the selectivity of PPK28 altered the conductance of the pressure-gated currents. The shift in ion selectivity strongly argues that the PPK28 channel carries the force-gated current.

Are domains of PPK28 are involved in sensing mechanical force? All Deg/ENaC proteins share similar topographic features, including two transmembrane domains, a variable external domain, and two short intracellular termini (Eastwood, AL., 2012). PPK28 may sense mechanical force through coupling to extracellular or intracellular components, by interacting with the lipid bilayer, or by another mechanism. To examine if specific domains of PPK28 are critical for gating, we generated chimeric proteins in which the N- and C- cytoplasmic domains of PPK28 and PPK23 were swapped (Fig. 4C) Surprisingly, the PPK23 core channel flanked by PPK28 termini (PPK28-23-28) showed calcium responses to hypotonic perfusion (Fig. 4D), whereas the PPK28 core channel flanked by PPK23 termini (PPK23-28-23) did not. Moreover, the individual C-terminal or N-terminal domain of PPK28 was not sufficient to confer osmosensitivity. Therefore, the PPK28 termini are likely the site at which changes in membrane tension are detected. Interestingly, these results are reminiscent of studies in the bacterial MscL channel and the mammalian stretch-sensitive two pore potassium channel TREK-1, both of which require their C-termini for mechanical sensitivity (Deadman, A. et al., 2008; Martinac, B., 2011).

Conclusion

Although mechanosensitive currents have been observed in diverse cell types, including bacteria, somatosensory neurons, frog oocytes, inner ear hair cells, muscle spindle fibers, and baroreceptors, few channels have been shown to be directly stretch-activated. Many candidate mechanosensory channels fail to be expressed or mechanically gated in heterologous systems, precluding functional studies (Geffney, SL. and Goodman, M. 2012). Our findings that PPK28 confers pressure sensitivity to heterologous cells, the pore carries the mechanically-gated current, and specific domains transfer pressure sensitivity onto another PPK, argues that PPK28 directly senses mechanical force. PPK28 does not require additional subunits or specialized accessory proteins to detect pressure, indicating that it may be directly gated by changes in the membrane bilayer rather than by intracellular or extracellular tethers. The biological role of PPK28 is for gustatory detection of water, consistent with the notion that it is activated by membrane swelling rather than by shear force. Our studies demonstrate that the osmosensitive PPK28 channel is activated by membrane tension and provide a framework for examining mechanical gating of the Deg/ENaC channel family.

Materials and Methods

Cell culture and transient transfection

All cultures were maintained in humidified incubators at 37°C with 5% CO_2. HEK293T cells were grown in Dulbecco's Modified Eagle Medium (Gibco) with 10% Fetal Bovine Serum, 50mg/ml^{-1} penicillin and 50mg/ml^{-1} streptomycin. CHO cells were grown in Ham's F-12 Nutrient Media (Gibco) with 10% Fetal Bovine Serum, 50mg/ml^{-1} penicillin and 50mg/ml^{-1} streptomycin. Ng108 cells were grown in [need buffer]. Cell cultures were plated on glass cover slips coated with Poly-D lysine (Millipore) and laminin (Sigma) for 12-24 hours and transfected using lipofectamine 2000 (Invitrogen) as instructed. All genetic constructs were transfected at a concentration of 500-1000 ng/$^{ml-1}$ and imaging and electrophysiological assays were performed 12-24 hours later. Co-transfection with *GFP* or *dsRed* at 300ng/ml^{-1} was used to identify cells in all imaging and electrophysiological experiments.

Calcium Imaging

Calcium imaging in osmotic stress experiments were performed as described, using the calcium indicator Fluo-4 (Invitrogen) and a confocal laser scanning microscope (Zeiss LSM510, Carl Zeiss) [cite Peter]. Before imaging, cells were loaded with 10μM Fluo-4 at 37°C for one hour in isotonic buffer containing (in mM) 76 NaCl, 5 KCl, 2 $MgCl_2$, 2 mM $CaCl_2$, 10 glucose, 10 HEPES, mannitol, pH 7.4). Varying mannitol achieved a low osmolality test buffer. Osmolality was determined by a vapor pressure osmometer (Vapro 5520, Wescor Inc.)

Cells were washed in isotonic solution three times following loading. They were set in a perfusion chamber and bathed in either isotonic or low osmotic solution. Fluorescence emission at 480nm was filtered using a 505-530 band pass filter. Analysis was performed using custom Mat Lab scripts.

Radial Stretch

Stretch assays were modified from. Circular membranes were punched from sheets of glossy silicone at a thickness of 0.01 inch. Membranes were coated with 20mg/ml^{-1} laminin prior to cell plating. Transfected cells were plated in the center of membranes overnight at 37°C and assayed 12-24 hours later. Cells were loaded with either Fluo-4 as described above or with 10uM Fura 2AM (Invitrogen) with 0.02% Pluronic F-127 (Invitrogen) to perform ratiometric calcium imaging.

Membranes were carefully mounted onto a StageFlexer system as instructed (Flexcell). Negative pressure was applied using an FX-3000 pump system. Cells were subjected to increasing negative pressure using a series of 2s square wave stimulations with an interval of 30s. These stimulations corresponded to radial stretch ranging from 0-25% of the silicone membrane. Following stretch, low osmotic solution was used as a positive control. For HEK293T experiments, ratiometric calcium imaging was used. Images were acquired as the ratio of 340nm to 380nm and aligned using MetaMorph software.

Electrophysiology

Patch-clamp experiments were performed in standard cell-attached or whole cell configurations using an Axopatch 200B amplifier (Axon Instruments). Patch pipets had resistances ranging from 2-5 MΩ. The extracellular solution consisted of (in mM) 127 NaCl, 3 KCl, 1 $MgCl_2$, 10 HEPES, 2.5 $CaCl_2$, 10 glucose (pH adjusted to 7.3 with NaOH). All experiments were performed at room temperature. Currents were sampled at 20kHz and filtered at 2kHz.

Cell attached recordings were performed as described (Coste et al, 2012). Pipets were filled with the following: (in mM) 130 NaCl, 5 KCl, 10 HEPES, 1 $CaCl_2$, 1$MgCl_2$, 10 TEA-Cl (pH 7.3 with NaOH). To zero the membrane potential external solution contained the following: (in mM) 140 KCl, 10 HEPES, 1 $MgCl_2$, 10 glucose (pH 7.3 with KOH).

GCaMP Imaging

In vivo calcium imaging was performed on single taste bristles on the proboscis as described [Thistle, R et al. 2012]. *UAS-GCaMP3* was targeted to water-sensitive taste neurons using the *ppk28-Gal4* driver. Taste bristles were encapsulated with a glass capillary for targeted stimulation lasting 30s. 20% polyethylene glycol was included to inhibit neural activity. Trinitrophenol stimulations ranged in concentration from 1nM-1mM.

Proboscis Extension Reflex Behavior

The Proboscis Extension Response (PER) was measured as previously described with modification [Mann, K. et al., 2013]. Flies of the following genotype were used: Δ*ppk28*, Δ*ppk28; UAS-ppk28; ppk28gal4*, and an isogenized genetic background control (Exelixis strain A5001, BL-6326). Female flies aged 3-5 days were collected and stored on fresh food one day prior to the experiment. Flies were mounted on glass slides using nail polish and desiccated for 2 hours in a sealed chamber containing 300-400g $CaSO_4$ (Hammond Drierite) to increase motivation for water. Flies were then stimulated on the proboscis with tastants and PER was measured in bins of ~20 flies per trial. All flies were reared on standard fly food.

Figure Legends

Figure 1. Cells expressing PPK28 respond to radial stretch

A. HEK293T cells loaded with Fluo-4. Cells that express PPK28 respond to low osmotic solutions. Representative ΔF/F heat maps for cells perfused with isotonic (300 mmol kg-1) or low osmotic (160 mmol kg-1) solutions. ΔF/F range is 0-70%. Scale bar, 40μM.

B. The ENaC blocker amiloride blocks osmosensation by PPK28 expressing cells. ΔF/F mean ± SEM. n = 4 - 6 trials. * $p < 0.05$, ** $p < 0.01$, student's t-test.

C. The osmosensation by PPK28 is not blocked by the TRP channel blocker ruthenium red, the voltage-sensitive calcium channel blocker gadolinium, or the potassium channel blocker NMDG. Chelation of bath calcium by EGTA abolishes PPK28 calcium responses to low osmotic solution. ΔF/F mean ± SEM. n = 4 - 6 trials. * $p < 0.05$, ** $p < 0.01$, student's t-test

D. Representative pseudocolor images of HEK293T cells loaded with the calcium indicator Fura-4AM. Cells that express PPK28 respond to 20% radial stretch as well as low osmotic solution. ΔF/F range is 0-70%. Scale bar, 40μM

E. Quantification of PPK28 expressing cells to increasing radial stretch. Cells respond in a dose dependent manner and this response is inhibited by amiloride. The related ion channel, PPK23, is not stretch sensitive. Normalized calcium response ± standard error of the mean (SEM). n = 4 -7 trials. * $p < 0.05$, ** $p < 0.01$, *** $p < 0.001$, student's t-test.

F. Functionality in multiple systems. PPK28 also confers stretch sensitivity when expressed in CHO and Ng108 cell lines. Normalized calcium responses ± SEM. n = 4 -5 trials. ** $p < 0.01$

Figure 2. The membrane crenator trinitrophenol activates cells and neurons expressing PPK28 contributing to behavior

A. Schematic of chemical manipulation of the cellular membrane. The molecules chlorpromazine and trinitrophenol insert into the inner and outter bilipid layer respectively, causing either concave or convex deformation.

B-C. HEK293T cells expressing PPK28 respond to increasing concentrations of trinitrophenol, but not to chlorpromazine. ΔF/F mean ± SEM. n = 3 – 5 trials ** $p < 0.01$

D. Proboscis neurons expressing *ppk28-gal4, UAS-GcamP3* respond to application of trinitrophenol. 20% PEG inhibits *ppk28-gal4* neural response to water. Addition of trinitriphenol to PEG solution is sufficient to activate neurons. This activation requires PPK28 as *Δppk28* flies fail to respond to water or trinitrophenol and this can be rescued by *ppk28-gal4* expression of *UAS-ppk28*. ΔF/F mean ± SEM. * $p < 0.05$, ** $p < 0.01$

E. Flies perform proboscis extension response (PER) to trinitrophenol. Desiccated female flies perform PER to water and 20% PEG inhibits this response. Addition of trinitriphenol to PEG

solution is sufficient to elicit PER. This behavior requires PPK28 as *Δppk28* flies fail to respond to water or trinitrophenol and this can be rescued by *ppk28-gal4* expression of *UAS-ppk28*. All flies perform PER to 100mM sucrose. n = 4 – 5 trials, 20 flies per genotype. ** $p < 0.01$

Figure 3. Cation currents are generated in PPK28 expressing cells upon negative pressure stimulation

A. Representative inward currents upon negative pressure application of HEK293T cells expressing either MPiezo or PPK28. Stimulus duration is 500ms and ranges from 0 – 70mmHg via cell attached HSPC system.

B. Cell attached peak currents recorded upon pressure stimulation of cells expressing MPiezo (13.34 ± 2.82pA) and PPK28 (9.97 ± 3.69pA). Addition of amiloride in the pipet blocks PPK28 currents but not MPiezo currents. Average peak current across all pressure stimulations ± SEM. n = 8 – 10 cells per condition. ** $p < 0.01$

C. I/V plot for HEK293T cells expressing PPK28. n = 7 cells.

D. Imax normalized current–pressure relationship of stretch-activated currents recorded at −80mV in PPK28 transfected cells (n = 6 cells) and fitted with a Boltzmann equation. P_{50} is the average of P_{50} values determined for individual cells.

Figure 4. PPK28 pore and termini mutations alter channel properties

A. The PPK28 pore residue mutation F499A alters the ion selectivity of PPK28. I/V curve shifts rightward approaching sodium selectivity. n = 8 cells.

B. Pore mutants fail to respond to hypotonic perfusion, consistent with a loss of calcium flux capacity. n = 4 – 6 trials.

C. Schematic of chimeric proteins generated using domains of PPK28 and PPK23. Domains swapped are the external domain including transmembrane domains 1 and 2 and the paired or single internal termini.

D. Of the chimeric proteins in (C), HEK293T cells expressing 28-23-28 respond to low osmotic solution. Other chimeric designs show no response.

Figure 1.

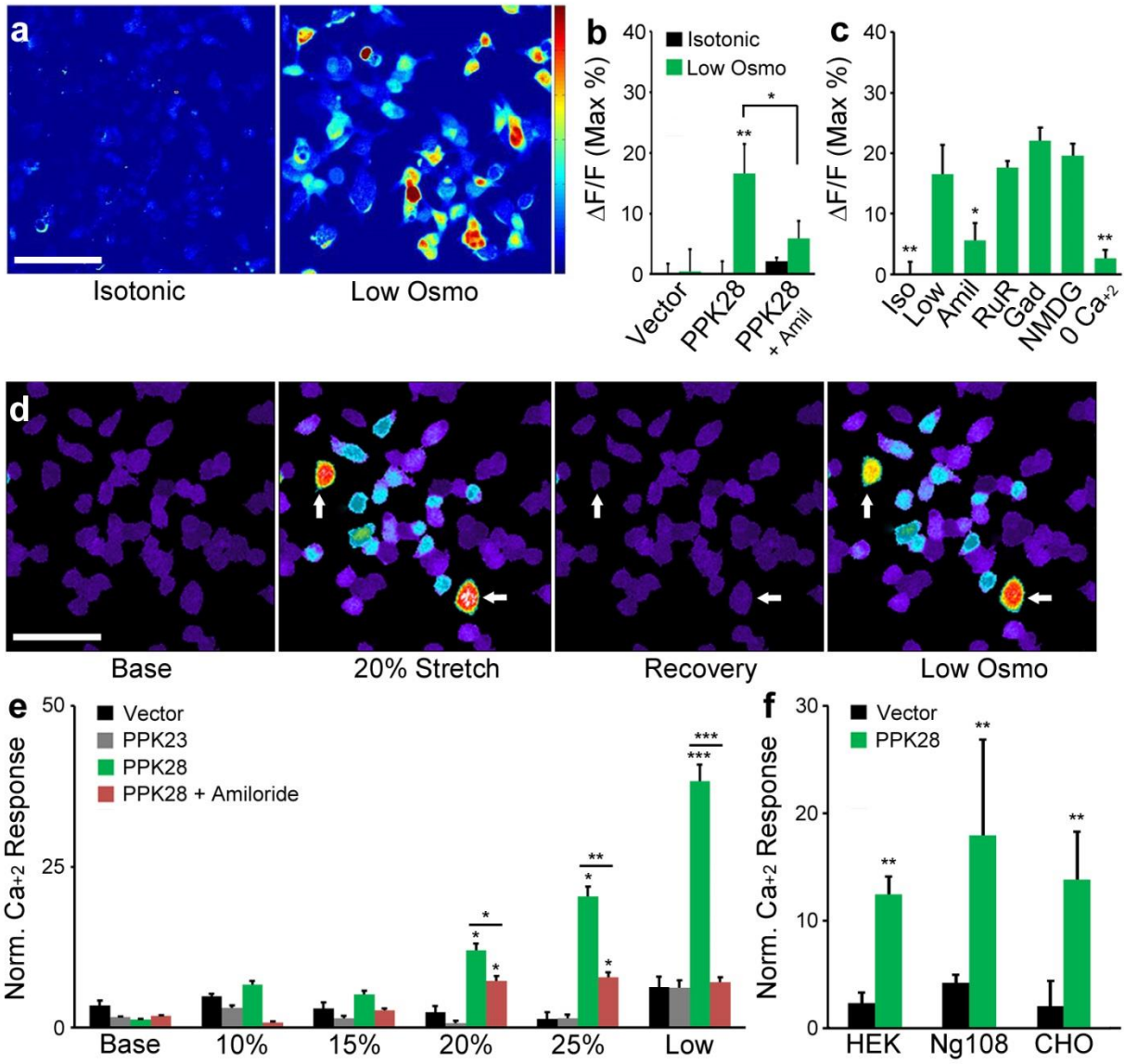
a
Isotonic
Low Osmo
b
Isotonic
Low Osmo
ΔF/F (Max %)
Vector
PPK28
PPK28 + Amil
c
ΔF/F (Max %)
Iso
Low
Amil
RuR
Gad
NMDG
0 Ca+2
d
Base
20% Stretch
Recovery
Low Osmo
e
Vector
PPK23
PPK28
PPK28 + Amiloride
Norm. Ca+2 Response
Base
10%
15%
20%
25%
Low
f
Vector
PPK28
Norm. Ca+2 Response
HEK
Ng108
CHO

Figure 2.

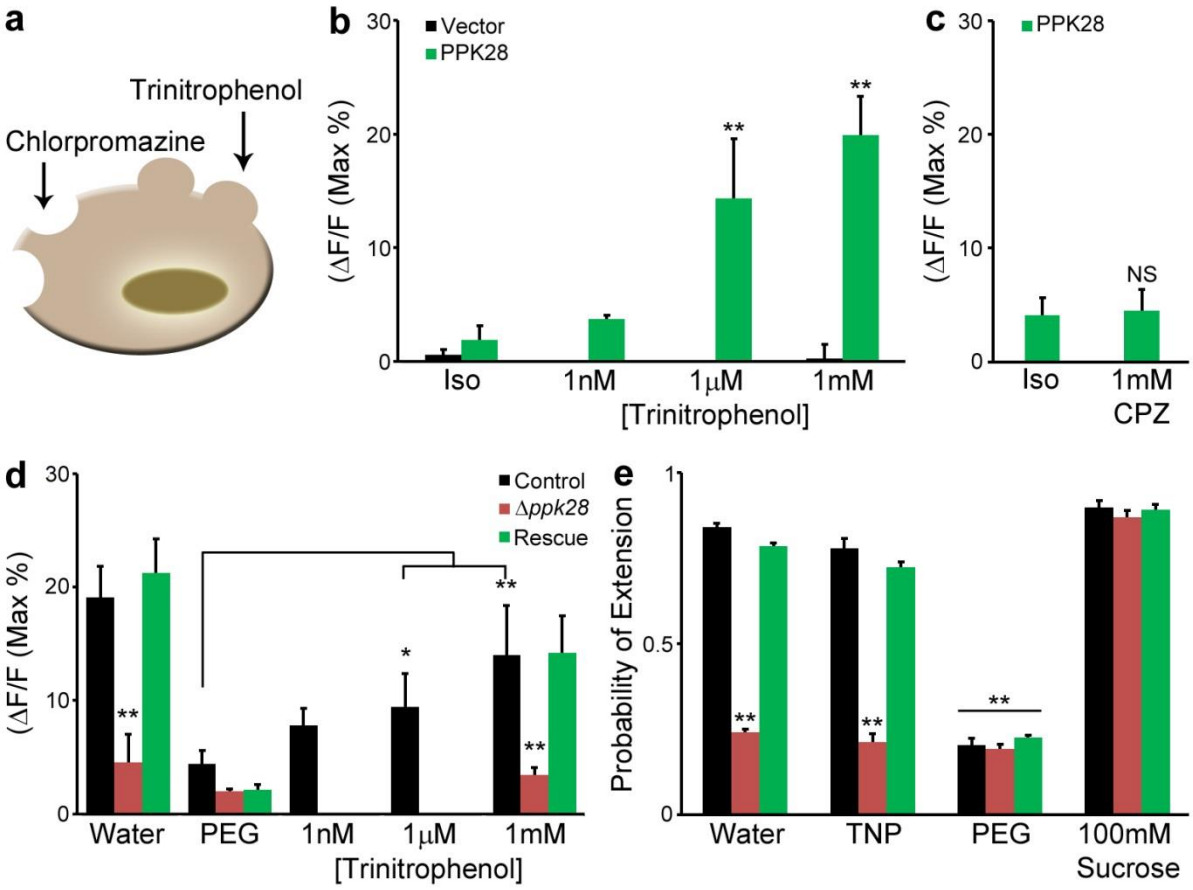
a
Trinitrophenol
Chlorpromazine
b
Vector
PPK28
(ΔF/F (Max %)
Iso
1nM
1μM
1mM
[Trinitrophenol]
c
PPK28
NS
Iso
1mM CPZ
d
Control
Δppk28
Rescue
Water
PEG
1nM
1μM
1mM
[Trinitrophenol]
e
Probability of Extension
Water
TNP
PEG
100mM Sucrose

Figure 3.

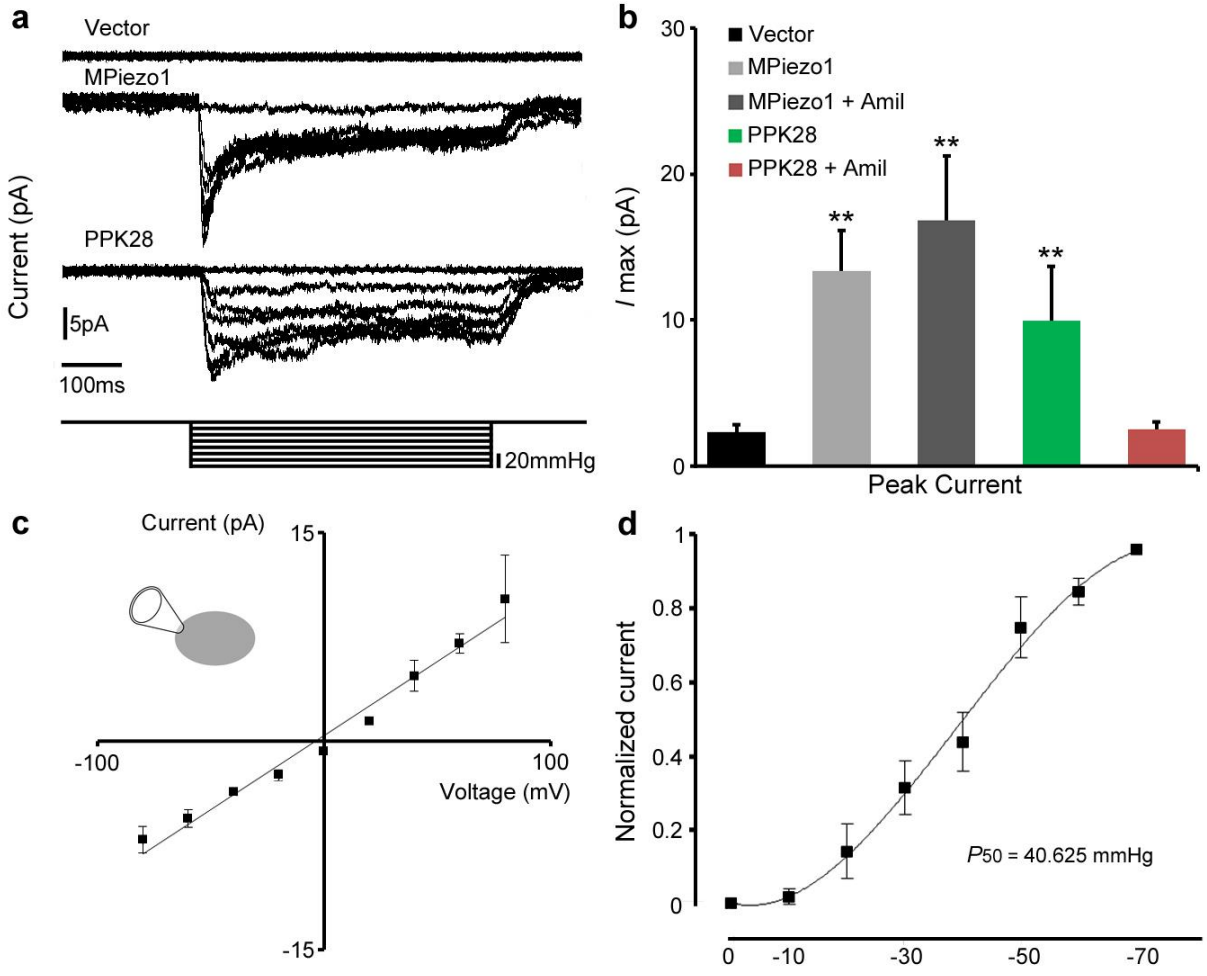
a
Vector
MPiezo1
PPK28
Current (pA)
5pA
100ms
20mmHg
b
Vector
MPiezo1
MPiezo1 + Amil
PPK28
PPK28 + Amil
I max (pA)
Peak Current
**
c
Current (pA)
15
-15
-100
100
Voltage (mV)
d
Normalized current
P50 = 40.625 mmHg
0
-10
-30
-50
-70

Figure 4.

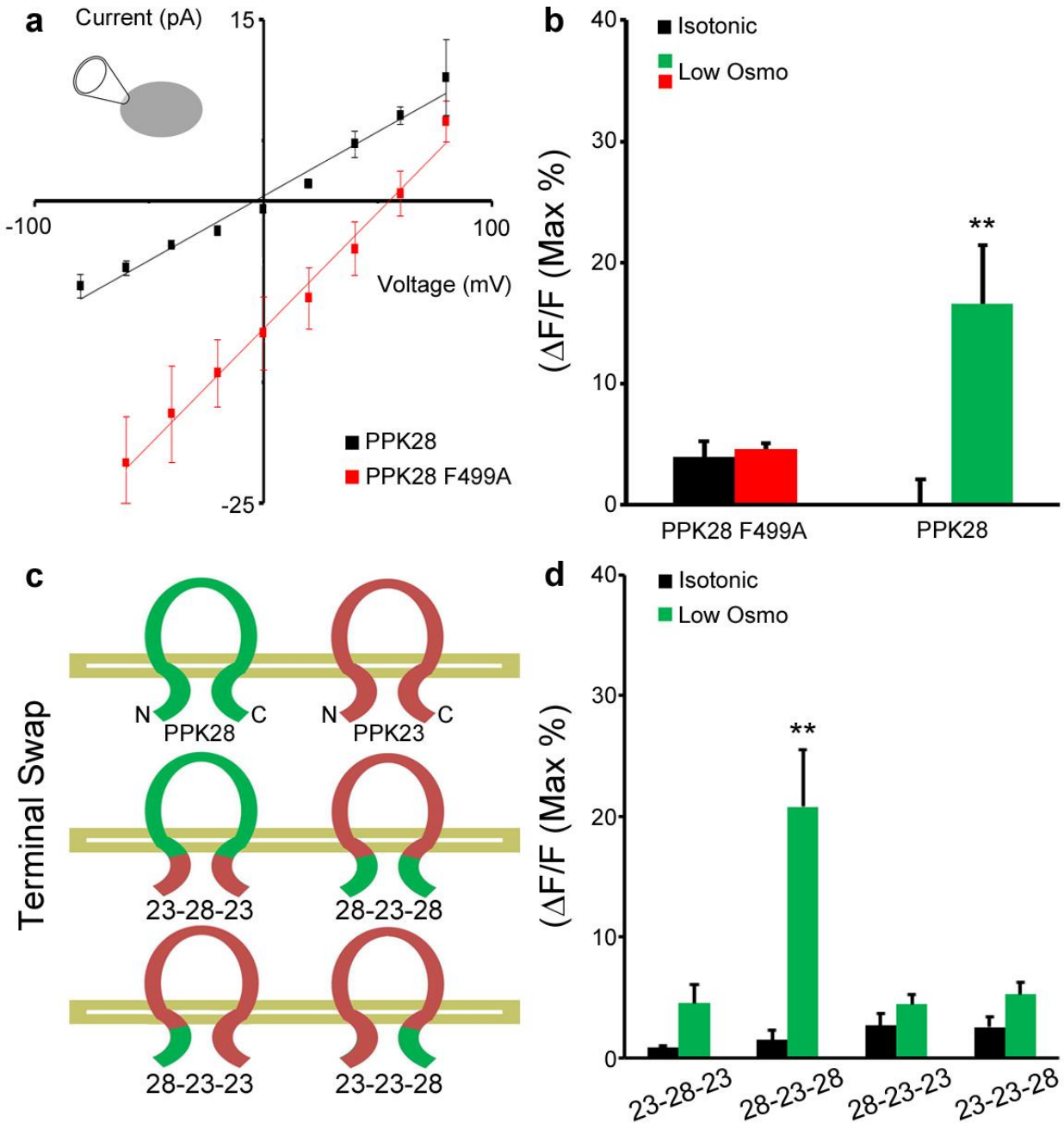
a
Current (pA)
15
-100
100
Voltage (mV)
-25
PPK28
PPK28 F499A
b
Isotonic
Low Osmo
(ΔF/F (Max %)
40
30
20
10
0
**
PPK28 F499A
PPK28
c
Terminal Swap
N
C
PPK28
PPK23
23-28-23
28-23-28
28-23-23
23-23-28
d
Isotonic
Low Osmo
(ΔF/F (Max %)
40
30
20
10
0
**
23-28-23
28-23-28
28-23-23
23-23-28

Supplemental Figure Legends

Figure S1. Increasing stretch yields sensitivity in more total cells, related to Figure 1.

A. The log of responding cells from all trials to increasing radial stretch. The number of responding cells transfected with PPK28 but not vector alone or PPK28 in the presence of amiloride increases with increasing stretch as indicated by a rightward shift in darker curves. Blue curves denote wash with low osmotic solution. n = 4-7 trials.

B. Percentage of total cells from (A) responding with a normalized calcium response greater than 10%. Increasing radial stretch of PPK28 cells (Figure 1D) causes an increased calcium response and also recruits a greater number of overall responding cells.

C. Representative traces of calcium responses of a PPK28 cell (black) and a PPK28 cell in the presence of amiloride (red) over time. Black dashes indicate periods of radial stretch.

Figure S2. Pore point mutation alters ion selectivity of PPK28, related to Figure 4.

Amino acid alignment of representative *Drosophila melanogaster* PPK ion channels. Colored sections are conserved portions of the transmembrane pore. The phenylalanine residue (green) of PPK28 is a site of ion selectivity, likely providing space within the pore for the flux of larger cations, unlike some Na^+ specific Deg/ENaCs. Alignments were generated using the ClustalW2 multiple sequence alignment program.

Supplemental Figure 1.

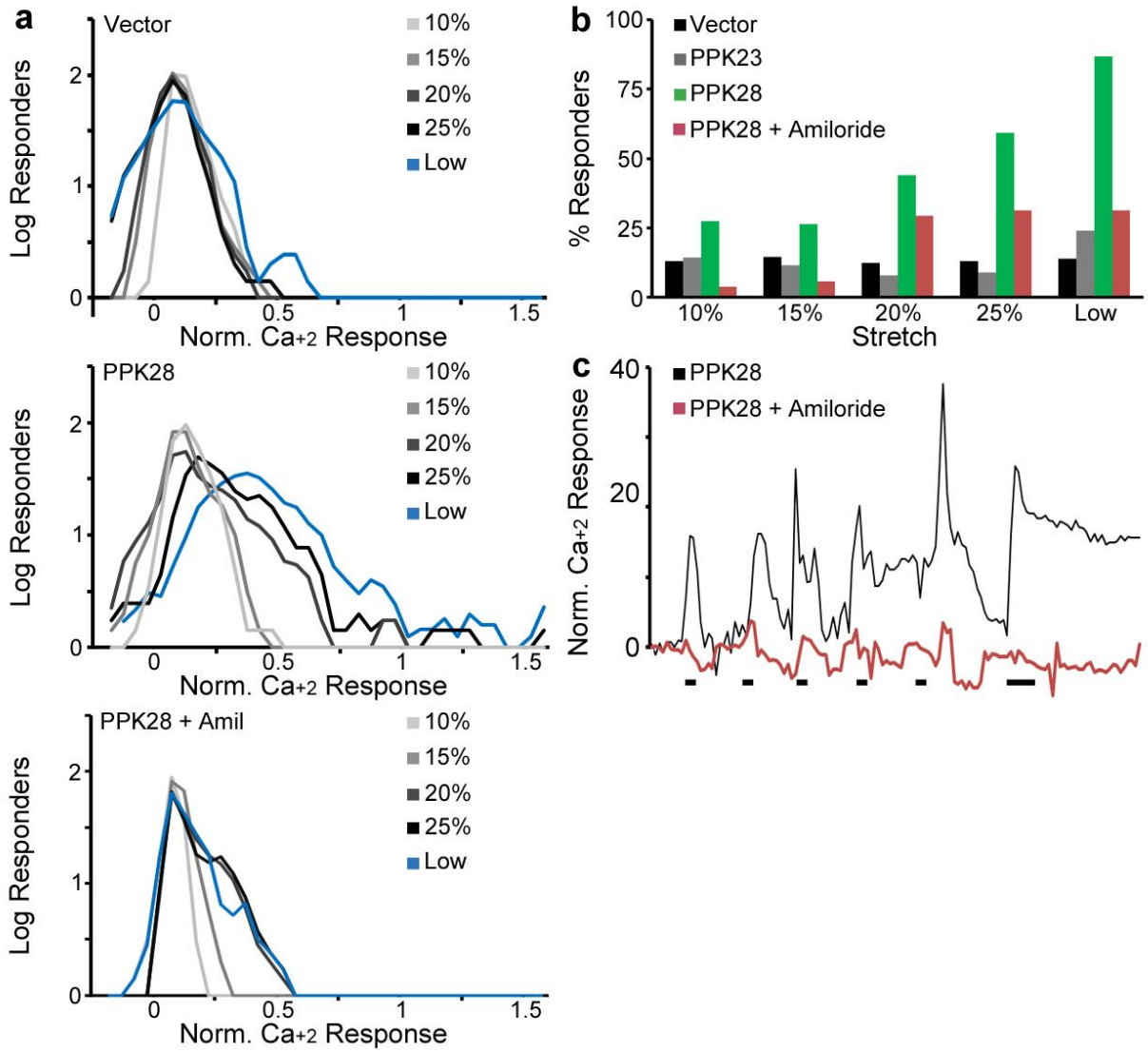

Supplemental Figure 2.

Chapter 4:

Discussion

PPKs Function in Courtship Behavior

Previous work implicated gustation as one of the sensory systems involved in *Drosophila* courtship. We utilized expression studies to verify that the pickpocket genes *ppk23* and *ppk29* are expressed exclusively in a novel population of taste neurons found in the proboscis, wing margins, and legs. Interestingly, expression of these genes overlaps with expression of the transcription factor *fruitless* in leg neurons. Moreover, projections from these leg neurons are sexually dimorphic in the ventral nerve cord, suggesting a role for these gustatory neurons during courtship behavior. Therefore we used genetic, conditional activation/inactivation, and calcium imaging to investigate the role of ion channels and taste neurons in pheromone detection and courtship behavior.

We show that *ppk23* is required for the correct sexual discrimination by males of courtship targets. Mutants court females less and other males more than their wild type siblings. Interestingly, *ppk29* mutations appear only to affect aspects of male-female courtship, suggesting that PPK23 cells may not be homogeneous in function. Activation and inactivation of these neurons enhances and abolishes courtship behavior contextually. For example, activating these cells when the courtship target is female causes males to court more. However, activating these cells when the courtship target is male causes males to court less. The inverse is true in neural silencing experiments. How can the taste system have both an "on" and "off" state working at the same time? One possibility is that males use other information from vision and olfaction in order to aid their courtship decision. Indeed, when males are placed in the dark with their antennae removed they will not court other flies even if PPK23 neurons are activated. Integration of multimodal stimuli likely yields to courtship inhibition, for example, even if the system receives "on" signals.

Calcium imaging experiments further demonstrate the heterogeneity of PPK23 neurons. On the legs, the neurons exist in pairs that innervate a single taste bristle. One of the neurons responds best to application of cuticular hydrocarbons found primarily on females while the other responds best to cuticular hydrocarbons found primarily on males. This difference in tuning at the sensory level provides a mechanism with which to probe the circuitry underlying courtship. Indeed, another pickpocket channel, PPK25 is expressed in only one of the two *fruitless* PPK23 neurons in each doublet. Previously, loss of this channel subunit affected only male-female courtship behavior, suggesting that PPK25 may be expressed in the neuron that responds best to female cuticular hydrocarbons. Using targeted GcamP expression in PPK25 cells, we show that these neurons do respond to female cuticular hydrocarbons, and that *ppk25* mutants do not, though they maintain the ability to detect male inhibitory pheromones. As a result, *ppk25* expression in what we call the "F cell" serves as a method to untangle the opponent signals received by PPK23 neurons.

Are pickpocket channels direct pheromone receptors or downstream molecules involved in changes of membrane potential? Our experiments have yet to reveal this answer. Misexpression studies in which PPK23, PPK29, and PPK25 are directed to empty gustatory neurons either as single units or in various combinations does not confer pheromone sensitivity. Moreover, reconstitution of these channels in heterologous systems does not confer pheromone sensitivity. However, as these genes cannot cross-rescue behavioral phenotypes in mutants, it is

likely that they perform a more direct role in pheromone detection. It may be that subunits partner in heterotrimers in which other subunits are not yet known. They may also require specific accessory binding proteins to traffic fatty pheromone molecules either on the surface or in the extracellular fluids of sensory bristles. Identifying other pickpocket channels expressed in leg sensory neurons will likely provide insight into this question.

How might PPK23 circuits be arranged? One simple explanation given the opponent signals that the sensory neurons detect is that it may be overall sensory activity that initiates one half of the circuit while suppressing the opposite half. This is reminiscent of non-synaptic lateral inhibition of olfactory neurons in *Drosophila*. The Carlson group performed simultaneous tip recordings on paired olfactory neurons and demonstrated that transient activation of one neuron will inhibit the sustained activity of its neighbor. Another model may involve circuit separation in the ventral nerve cord or brain following sensory activation. For example, activation of the F cell may activate downstream second order neurons which inhibit or dampen components of the circuit that are downstream of the male pheromone sensing cell, or "M cell." Exciting ongoing work investigates this possibility using artificial sensory activation and whole brain calcium imaging. It will be interesting to see how the opponent circuits affect one another's activity and whether or not they impinge on higher order components of the *fruitless* olfactory circuit to produce an ultimate behavior.

PPK28 Links Osmosensation to Mechanosensation

The Deg/ENaC family of proteins has been implicated in the detection of multiple stimuli including acids, sodium, peptides, osmolarity, and mechanical force. Despite extensive studies, the underlying molecular mechanisms for these detections are still poorly understood. Recently, much attention has been given to proteins like TRPs, Piezos, and TMCs as being bona fide mechanotransduction channels. The *Drosophila* TRP protein NOMPC, expressed in larval multidendritic neurons is required for gentle touch behavior responses and can confer mechanosensitivity to heterologous cells. Mammalian Piezo proteins, expressed in various tissues (Piezo1 in lungs, bladder, skin; Piezo2 in dorsal root ganglia, merkel cells) can similarly conduct pressure-evoked currents in a variety of heterologous systems. These large multipass transmembrane proteins also detect noxious pressure in *Drosophila* larvae. However, given their size, they are difficult to study biophysically and the putative pore domain is not known. Finally, two TMC (Transmembrane channel-like 1 and 2) are expressed in mammalian auditory and vestibular hair cells. Whole cell and single channel recordings from these cells show pressure evoked currents dependent on these genes. Further, mutants display deafness and/or vestibular defects. How do these channels convert force into current? Gating of mechanically sensitive channels remains an open question in channel physiology and these candidates represent exciting new avenues to explore this mechanism.

Although there has been a huge push toward understanding ion channels that directly sense mechanical force, less attention has been given to Deg/ENaCs. Compelling evidence for their role in mechanosensation comes from *C. elegans*. Two Deg/ENaCs, MEC-4 and MEC-10, form the pore of a mechanically sensitive channel in conjunction with accessory proteins *in vivo*. This channel complex underlies gentle touch escape behavior. Unfortunately, the requirement of multiple units for function has made channel gating studies challenging. In *Drosophila*, other

Deg/ENaCs have also been implicated in mechanosensation. Multidendritic neurons that tile the larval body wall and respond to touch express multiple PPKs as well as dmPiezo. Exciting new work shows that PPK1 and PPK26 are coexpressed in these cells, interdependent on membrane localization, and required for noxious mechanical nociception. These data suggest the intriguing possibility that these subunits form a functional heteromeric channel, similar to our hypothesis of heteromeric partnering of PPKs in pheromone sensing neurons.

The role of osmosenstion by PPK28 provides an excellent platform with which to study the gating of Deg/ENaCs. Our data demonstrate that PPK28 can function alone. Misexpression both in taste neurons and in multiple heterologous systems confers osmosensitivity. The channel is also stretch sensitive, opened by chemical manipulation of the cellular membrane, and carries pressure-derived current. Given the smaller size and relatively simple architecture of PPK28 compared to TRPs, Piezos, and TMCs, we were able to probe regions of the protein for functionality. Domain swapping experiments point to the protein termini as critical sites for stretch sensitivity. The amphipathic properties of these residues may allow PPK28 to interact directly with the cellular membrane to sense curvature or tension, bypassing the need for accessory proteins or binding partners in the extracellular matrix and cytoskeleton. Moreover, mutagenesis of pore residues changes the ion selectivity of the channel, arguing that PPK28 carries the observed pressure-derived current.

Our data show that Deg/ENaCs can be directly gated by mechanical force. Pickpocket ion channel subunits share high levels of protein similarity, suggesting that this mechanism of gating may be conserved. Many cells carry mechanically induced currents without identified molecular transducers or amplifiers. Future studies may reveal that other Deg/ENaCs serve a more fundamental role in peripheral and central osmosensation, touch, pain, and audition. The challenge, perhaps, has been in identifying functional channels comprised of multiple units. It will be interesting to see if more heteromeric stretch sensitive channels are uncovered. How are subunit partners determined? How functionally redundant are subunits? What role, if any, do the extensive extracellular loops play in gating or transduction?

References

Adams, C.M., Anderson, M.G., Motto, D.G., Price, M.P., Johnson, W.A., and Welsh, M.J. (1998). Ripped pocket and pickpocket, novel Drosophila DEG/ENaC subunits expressed in early development and in mechanosensory neurons. J Cell Biol *140*, 143-152.

Antony, C., and Jallon, M. (1982). The chemical basis for sex recognition in Drosophila melanogaster. J Insect Physiology *28*, 87-880.

Bhattacharya MRC, Bautista DM, Wu K, Haeberle H, Lumpkin EA, Julius D. Radial stretch reveals distinct populations of mechanosensitive mammalian somatosensory neurons. Proceedings of the National Academy of Sciences of the United States of America 2008;105(50):20015-20020. doi:10.1073/pnas.0810801105

Ben-Shahar, Y., Lu, B., Collier, D.M., Snyder, P.M., Schnizler, M., and Welsh, M.J. (2010). The Drosophila gene CheB42a is a novel modifier of Deg/ENaC channel function. PloS one *5*, e9395.

Benton, R., Vannice, K.S., Vosshall, L.B. (2007). An essential role for a CD36-related receptor in pheromone detection in Drosophila. Nature *450*, 289-93.

Benton, R., Vannice, K.S., Gomez-Diaz, C., Vosshall, L.B. (2009). Variant ionotropic glutamate receptors as chemosensory receptors in Drosophila. Cell *136*, 149-62.

Billeter, J.C., Atallah, J., Krupp, J.J., Millar, J.G., and Levine, J.D. (2009). Specialized cells tag sexual and species identity in Drosophila melanogaster. Nature *461*, 987-991.

Bray, S., and Amrein, H. (2003). A putative Drosophila pheromone receptor expressed in male-specific taste neurons is required for efficient courtship. Neuron *39*, 1019-1029.

Brown AL, Fernandez-Illescas SM, Liao Z, Goodman MB. Gain-of-Function Mutations in the MEC-4 DEG/ENaC Sensory Mechanotransduction Channel Alter Gating and Drug Blockade. The Journal of General Physiology 2007;129(2):161-173. doi:10.1085/jgp.200609672.

Buck, L. and Axel, R. (1991). A novel multigene family may encode odorant receptors: a molecular basis for odor recognition. Cell *65,* 175-87

Butterworth, F.M. (1969). Lipids of Drosophila: a newly detected lipid in the male. Science (New York, NY *163*, 1356-1357.

Colbert, H. A., Smith, T. L. and Bargmann, C. I. (1997). OSM-9, a novel protein with structural similarity to channels, is required for olfaction, mechanosensation, and olfactory adaptation in Caenorhabditis elegans. J Neurosci *17*, 8259-8269.

Coste, B., Xiao, B., Santos, J. S., Syeda, R., Grandl, J., Spencer, K. S., Patapoutian, A. (2012). Piezos are pore-forming subunits of mechanically activated channels. Nature, 483(7388), 176–181. doi:10.1038/nature10812

Choi S-Y, Kim Y-H, Lee Y-K, Kim K-T. Chlorpromazine inhibits store-operated calcium entry and subsequent noradrenaline secretion in PC12 cells. British Journal of Pharmacology 2001;132(2):411-418. doi:10.1038/sj.bjp.0703840.

Cameron, P., Hiroi, M., Ngai, J., and Scott, K. (2010). The molecular basis for water taste in Drosophila. Nature *465*, 91-95.

Chandrashekar, J., Hoon, M.A., Ryba, N.J., Zuker, C.S. (2006). The receptors and cells for mammalian taste. Nature *444*, 288-94.

Chandrashekar, J., Kuhn, C., Oka, Y., Yarmolinsky, D.A., Hummler, E., Ryba, N.J., Zuker, C.S. (2010). The cells and peripheral representation of sodium taste in mice. Nature *464*, 297-301.

Chen, Z., Wang, Q., and Wang, Z. (2010). The amiloride-sensitive epithelial Na+ channel PPK28 is essential for drosophila gustatory water reception. J Neurosci *30*, 6247-6252.

Chyb, S., Dahanukar, A., Wickens, A., and Carlson, J.R. (2003). Drosophila Gr5a encodes a taste receptor tuned to trehalose. Proceedings of the National Academy of Sciences of the United States of America *100 Suppl 2*, 14526-14530.

Clyne, P.J., Warr, C.G., Carlson, J.R. (2000). Candidate taste receptors in Drosophila. Science *287*, 1830-4.

Dahanukar, A., Lei, Y.T., Kwon, J.Y., and Carlson, J.R. (2007). Two gr genes underlie sugar reception in Drosophila. Neuron *56*, 503-516.

Datta, S.R., Vasconcelos, M.L., Ruta, V., Luo, S., Wong, A., Demir, E., Flores, J., Balonze, K., Dickson, B.J., and Axel, R. (2008). The Drosophila pheromone cVA activates a sexually dimorphic neural circuit. Nature *452*, 473-477.

Demir, E., and Dickson, B.J. (2005). fruitless splicing specifies male courtship behavior in Drosophila. Cell *121*, 785-794.

Eastwood AL, Goodman MB. Insight into DEG/ENaC Channel Gating from Genetics and Structure. Physiology (Bethesda, Md.) 2012;27(5):282-290. doi:10.1152/physiol.00006.2012.

Ejima, A., and Griffith, L.C. (2008). Courtship initiation is stimulated by acoustic signals in Drosophila melanogaster. PloS one *3*, e3246.

Everaerts, C., Farine, J.P., Cobb, M., and Ferveur, J.F. (2010). Drosophila cuticular hydrocarbons revisited: mating status alters cuticular profiles. PloS one *5*, e9607.

Falk, R., Bleiser-Avivi, N., and Atidia, J. (1976). Labellar Taste Organs of Drosophila Melanogaster. Journal of Morphology *150*, 327-341.

Fang J, Iwasa KH. Effects of Chlorpromazine and Trinitrophenol on the Membrane Motor of Outer Hair Cells. Biophysical Journal 2007;93(5):1809-1817. doi:10.1529/biophysj.106.100834.

Ferveur, J.F. (2005). Cuticular hydrocarbons: their evolution and roles in Drosophila pheromonal communication. Behavior genetics *35*, 279-295.

Ferveur, J.F., Savarit, F., O'Kane, C.J., Sureau, G., Greenspan, R.J., and Jallon, J.M. (1997). Genetic feminization of pheromones and its behavioral consequences in Drosophila males. Science (New York, NY *276*, 1555-1558.

Fischler, W., Kong, P., Marella, S. and Scott, K. (2007). The detection of carbonation by the Drosophila gustatory system. Nature *448*, 1054-1057.

Fishilevich, E., and Vosshall, L.B. (2005). Genetic and functional subdivision of the Drosophila antennal lobe. Curr Biol *15*, 1548-1553.

Gailey, D.A., Jackson, F.R., and Siegel, R.W. (1984). Conditioning Mutations in DROSOPHILA MELANOGASTER Affect an Experience-Dependent Behavioral Modification in Courting Males. Genetics *106*, 613-623.

Geffeney SL, Goodman MB. How we feel: Ion channel partnerships that detect mechanical inputs and give rise to touch and pain perception. Neuron 2012;74(4):609-619. doi:10.1016/j.neuron.2012.04.023.

Gill, K.S. (1963). A mutation causing abnormal courtship and mating behavior in males of Drosophila melanogaster. American Zoology *3*, 507.

Goodwin, S.F., Taylor, B.J., Villella, A., Foss, M., Ryner, L.C., Baker, B.S., and Hall, J.C. (2000). Aberrant splicing and altered spatial expression patterns in fruitless mutants of Drosophila melanogaster. Genetics *154*, 725-745.

Greenspan, R.J. (1995). Understanding the genetic construction of behavior. Scientific American *272*, 72-78.

Greenspan, R.J., and Ferveur, J.F. (2000). Courtship in Drosophila. Annual review of genetics *34*, 205-232.

Hall, J.C. (1978). Courtship among males due to a male-sterile mutation in Drosophila melanogaster. Behavior genetics *8*, 125-141.

Hall, J.C. (1994). The mating of a fly. Science (New York, NY *264*, 1702-1714.

Hamada, F.N., Rosenzweig, M., Kang, K., Pulver, S.R., Ghezzi, A., Jegla, T.J., and Garrity, P.A. (2008). An internal thermal sensor controlling temperature preference in Drosophila. Nature *454*, 217-220.

Hiroi, M., Meunier, N., Marion-Poll, F. and Tanimura, T. (2004). Two antagonistic gustatory receptor neurons responding to sweet-salty and bitter taste in Drosophila. J Neurobiol *61*, 333-342.

Ito, H., Fujitani, K., Usui, K., Shimizu-Nishikawa, K., Tanaka, S., and Yamamoto, D. (1996). Sexual orientation in Drosophila is altered by the satori mutation in the sex-determination gene fruitless that encodes a zinc finger protein with a BTB domain. Proceedings of the National Academy of Sciences of the United States of America *93*, 9687-9692.

Jallon, J.M. (1984). A few chemical words exchanged by Drosophila during courtship and mating. Behavior genetics *14*, 441-478.

Kellenberger S, Schild L (2002) Epithelial sodium channel/degenerin family of ion channels: a variety of functions for a shared structure. Physiol Rev 82:735–767

Krstic, D., Boll, W., and Noll, M. (2009). Sensory integration regulating male courtship behavior in Drosophila. PloS one *4*, e4457.

Lai, S.L., and Lee, T. (2006). Genetic mosaic with dual binary transcriptional systems in Drosophila. Nature neuroscience *9*, 703-709.

Lee, G., Foss, M., Goodwin, S.F., Carlo, T., Taylor, B.J., and Hall, J.C. (2000). Spatial, temporal, and sexually dimorphic expression patterns of the fruitless gene in the Drosophila central nervous system. Journal of neurobiology *43*, 404-426.

Lee, T., and Luo, L. (1999). Mosaic analysis with a repressible neurotechnique cell marker for studies of gene function in neuronal morphogenesis. Neuron *22*, 451-461.

Lin, H., Mann, K.J., Starostina, E., Kinser, R.D., and Pikielny, C.W. (2005). A Drosophila DEG/ENaC channel subunit is required for male response to female pheromones. Proceedings of the National Academy of Sciences of the United States of America *102*, 12831-12836.

Liu, L., Johnson, W.A., and Welsh, M.J. (2003a). Drosophila DEG/ENaC pickpocket genes are expressed in the tracheal system, where they may be involved in liquid clearance. Proceedings of the National Academy of Sciences of the United States of America *100*, 2128-2133.

Liu, L., Leonard, A.S., Motto, D.G., Feller, M.A., Price, M.P., Johnson, W.A., and Welsh, M.J. (2003b). Contribution of Drosophila DEG/ENaC genes to salt taste. Neuron *39*, 133-146.

Mano, I., and Driscoll, M. (1999). DEG/ENaC channels: a touchy superfamily that watches its salt. Bioessays *21*, 568-578.

Manoli, D.S., Foss, M., Villella, A., Taylor, B.J., Hall, J.C., and Baker, B.S. (2005). Male-specific fruitless specifies the neural substrates of Drosophila courtship behaviour. Nature *436*, 395-400.

Marella, S., Fischler, W., Kong, P., Asgarian, S., Rueckert, E. and Scott, K. (2006). Imaging taste responses in the fly brain reveals a functional map of taste category and behavior. Neuron *49*, 285-295.

Martinac, B. Bacterial Mechanosensitive Channels as a Paradigm for Mechanosensory Transduction. Cell Physiol Biochem 2011;28:1051-1060

Mellert, D.J., Knapp, J.M., Manoli, D.S., Meissner, G.W., and Baker, B.S. (2010). Midline crossing by gustatory receptor neuron axons is regulated by fruitless, doublesex and the Roundabout receptors. Development (Cambridge, England) *137*, 323-332.

Miyamoto, T., and Amrein, H. (2008). Suppression of male courtship by a Drosophila pheromone receptor. Nature neuroscience *11*, 874-876.

Moon, S.J., Lee, Y., Jiao, Y., and Montell, C. (2009). A Drosophila gustatory receptor essential for aversive taste and inhibiting male-to-male courtship. Curr Biol *19*, 1623-1627.

Oka, Y., Omura, M., Kataoka, H., Touhara, K. (2004). Olfactory receptor antagonism between odorants. EMBO *23*: 120-6

Park, S.K., Mann, K.J., Lin, H., Starostina, E., Kolski-Andreaco, A., and Pikielny, C.W. (2006). A Drosophila protein specific to pheromone-sensing gustatory hairs delays males' copulation attempts. Curr Biol *16*, 1154-1159.

Parks, A.L., Cook, K.R., Belvin, M., Dompe, N.A., Fawcett, R., Huppert, K., Tan, L.R., Winter, C.G., Bogart, K.P., Deal, J.E., *et al.* (2004). Systematic generation of high-resolution deletion coverage of the Drosophila melanogaster genome. Nature genetics *36*, 288-292.

Ruta, V., Datta, S.R., Vasconcelos, M.L., Freeland, J., Looger, L.L., and Axel, R. (2010). A dimorphic pheromone circuit in Drosophila from sensory input to descending output. Nature *468*, 686-690.

Ryner, L.C., Goodwin, S.F., Castrillon, D.H., Anand, A., Villella, A., Baker, B.S., Hall, J.C., Taylor, B.J., and Wasserman, S.A. (1996). Control of male sexual behavior and sexual orientation in Drosophila by the fruitless gene. Cell *87*, 1079-1089.

Scott, K., 2005. Taste recognition: food for thought. Neuron *48*, 455-64.

Scott, K., Brady, R.J., Cravchik, A., Morozov, P., Rzhetsky, A., Zuker, C., and Axel, R. (2001). A chemosensory gene family encoding candidate gustatory and olfactory receptors in Drosophila. Cell *104*, 661-673.

Stocker, R.F. (1994). The organization of the chemosensory system in *Drosophila melanogaster*: a review. Cell Tissue Res *275*, 3-26.

Starostina E, Liu T, Vijayan V, Zheng Z, Siwicki KK, et al. (2012) A Drosophila DEG/ENaC Subunit Functions Specifically in Gustatory Neurons Required for Male Courtship Behavior. J Neurosci 32: 4665–4674. doi: 10.1523/jneurosci.6178-11.2012

Stockinger, P., Kvitsiani, D., Rotkopf, S., Tirian, L., and Dickson, B.J. (2005). Neural circuitry that governs Drosophila male courtship behavior. Cell *121*, 795-807.

Stowers, L., and Marton, T.F. (2005). What is a pheromone? Mammalian pheromones reconsidered. Neuron *46*, 699-702.

Sweeney, S., Broadie, K., Keane, J., Niemann, H., and O'Kane, C. (1995). Targeted expression of tetanus toxin light chain in Drosophila specifically eliminates synaptic transmission and causes behavioral defects. Neuron *14*, 341-351.

Thistle R, Cameron P, Ghorayshi A, Dennison L, Scott K (2012) Contact Chemoreceptors Mediate Male-Male Repulsion and Male-Female Attraction during Drosophila Courtship. Cell 149: 1140–1151. doi: 10.1016/j.cell.2012.03.045

Thorne, N., Chromey, C., Bray, S., and Amrein, H. (2004). Taste perception and coding in Drosophila. Curr Biol *14*, 1065-1079.

Tian L, Hires S, Mao T, Huber D, Chiappe M, et al. (2009) Imaging neural activity in worms, flies and mice with improved GCaMP calcium indicators. Nat Meth 6 (12) 875–81. doi: 10.1038/nmeth.1398

Vijayan, V., Thistle, R., Liu, T., Starostina, E., and Pikielny, C. (2014). Drosophila Pheromone-Sensing Neurons Expressing the ppk25 Ion Channel Subunit Stimulate Male Courtship and Female Receptivity. Plos Genetics. 10.1371

Villella, A., Gailey, D.A., Berwald, B., Ohshima, S., Barnes, P.T., and Hall, J.C. (1997). Extended reproductive roles of the fruitless gene in Drosophila melanogaster revealed by behavioral analysis of new fru mutants. Genetics *147*, 1107-1130.

Von Philipsborn, A.C., Liu, T., Yu, J.Y., Masser, C., Bidaye, S.S., and Dickson, B.J. (2011). Neuronal control of Drosophila courtship song. Neuron *69*, 509-522.

Vosshall, L.B. (2008). Scent of a fly. Neuron *59*, 685-689.

Vosshall, L.B., Wong, A.M., and Axel, R. (2000). An Olfactory Sensory Map in the Fly Brain. Cell *102*, 147-159.

Wang, L., Han, X., Mehren, J., Hiroi, M., Billeter, J.C., Miyamoto, T., Amrein, H., Levine, J.D., and Anderson, D.J. (2011). Hierarchical chemosensory regulation of male-male social interactions in Drosophila. Nature neuroscience *14*, 757-762.

Wang, Z., Singhvi, A., Kong, P., and Scott, K. (2004). Taste representations in the Drosophila brain. Cell *117*, 981-991.

Watanabe, K., Toba, G., Koganezawa, M., and Yamamoto, D. (2011). Gr39a, a Highly Diversified Gustatory Receptor in Drosophila, has a Role in Sexual Behavior. Behavior genetics.

Yarmolinsky, D. A., Zuker, C. S. and Ryba, N. J. (2009). Common sense about taste: from mammals to insects. Cell *139*, 234-244.

Yew, J.Y., Dreisewerd, K., Luftmann, H., Muthing, J., Pohlentz, G., and Kravitz, E.A. (2009). A new male sex pheromone and novel cuticular cues for chemical communication in Drosophila. Curr Biol *19*, 1245-1254.

Zhong, L., Hwang, R.Y., and Tracey, W.D. (2010). Pickpocket is a DEG/ENaC protein required for mechanical nociception in Drosophila larvae. Curr Biol *20*, 429-434.